Commissioning and initial results from the Super Fine Grained Detector (SFGD)

Tomislav Vladisavljevic, Rutherford Appleton Laboratory, UKRI
tomislav.vladisavljevic@stfc.ac.uk

On behalf of the T2K Collaboration
Given at 21st Recontres du Vietnam, 22-25 July 2025, ICISE, Quy Nhon, Vietnam

Science and Technology Facilities Council

Tokai-to-Kamioka (T2K) Experiment

International collaboration: 565 members from 75 institutions in 15 countries (as of 1 July 2025)

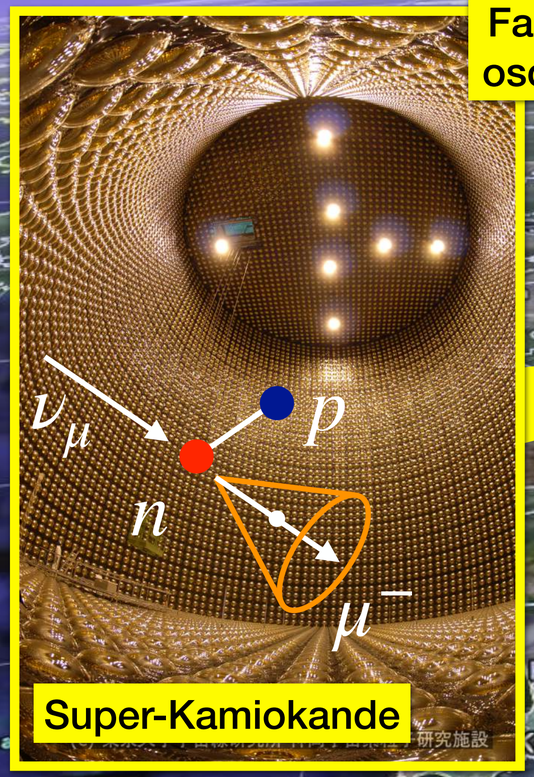

Far detector "measures" the oscillated beam composition

295 km baseline for neutrino oscillations

Upgrade completed in May 2024! (More in this talk)

Near Detector Complex aka ND280 (280 m from production) "measures" the initial beam composition

(Anti-)neutrino beam (~600 MeV) produced at J-PARC

Tomislav Vladisavljevic (tomislav.vladisavljevic@stfc.ac.uk)

Role of ND280 in oscillation analyses

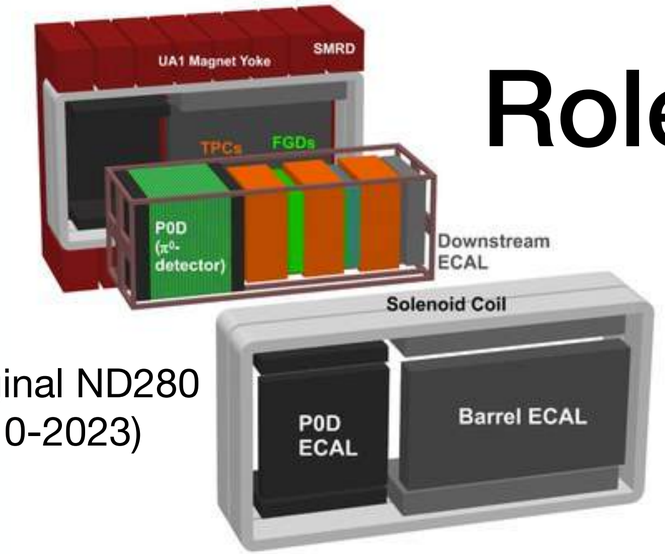

Original ND280
(2010-2023)

- In addition to providing the target material for a whole range of neutrino cross section measurements (more on this in the “Recent neutrino cross section results from T2K” talk on Thursday, ND280 is a crucial ingredient for oscillation measurements

- Fits to near detector data improve our predictive capabilities at Super-K, e.g. from 16.7% to 3.4% systematic uncertainty on the charged current induced pionless (CC0 π) ν_μ event rate

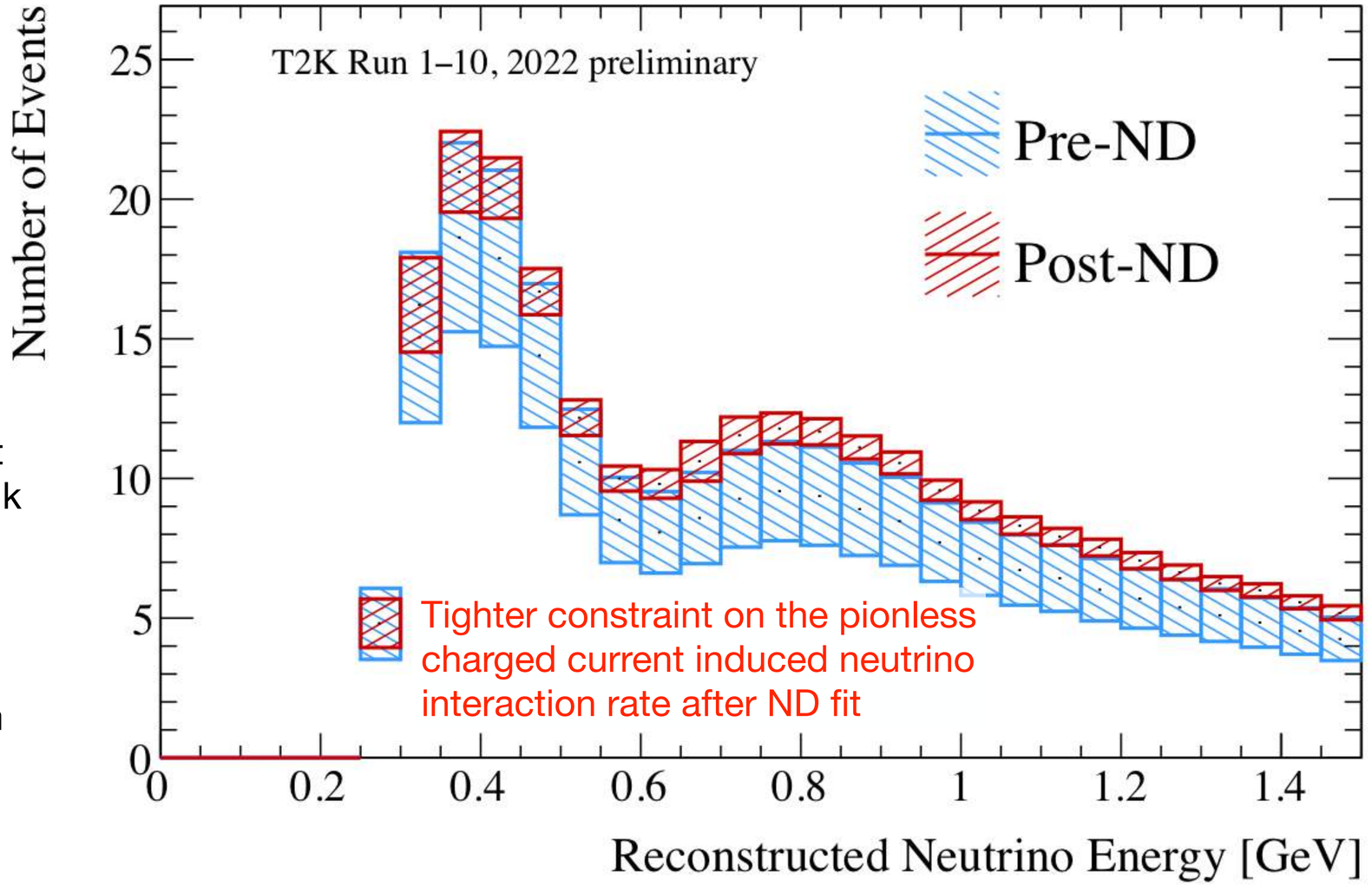

Limitations of the original ND280

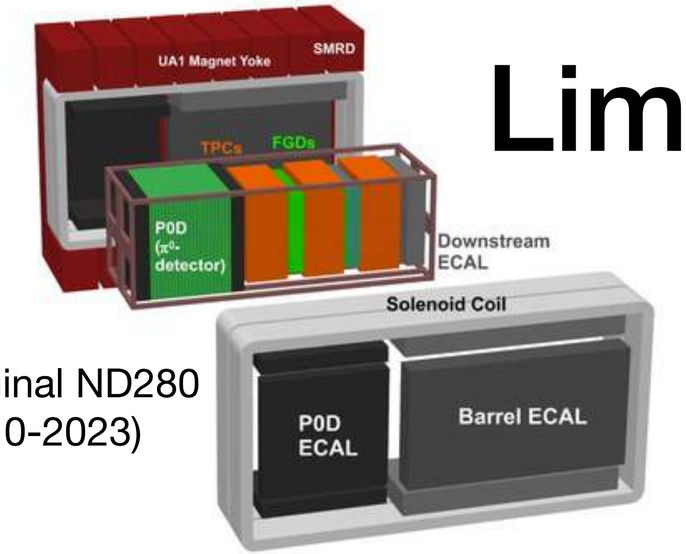

Original ND280
(2010-2023)

- The acceptance and reconstruction efficiency of the near detector don't quite match the phase space that contributes to oscillations at SK (far detector site)

- In particular:
  - Low selection efficiency for low momentum proton track reconstruction
  - Still have limited ability to match SK muon acceptance in high angle and backward going tracks with ND280 (due to absence of high angle TPCs)

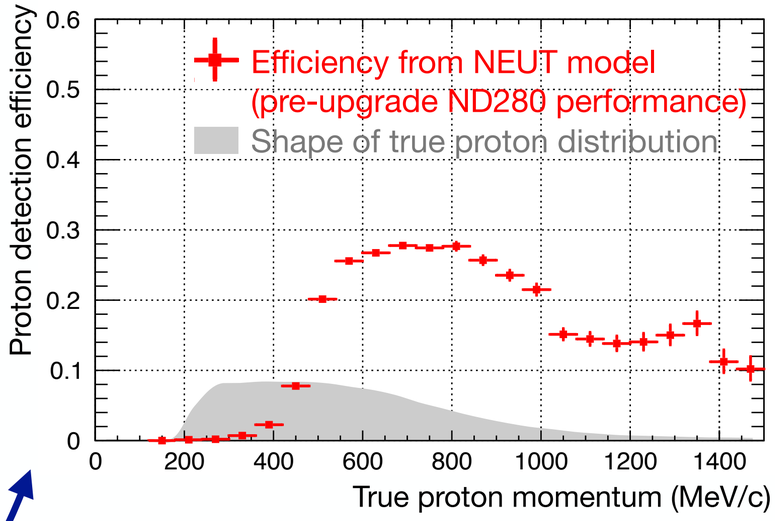

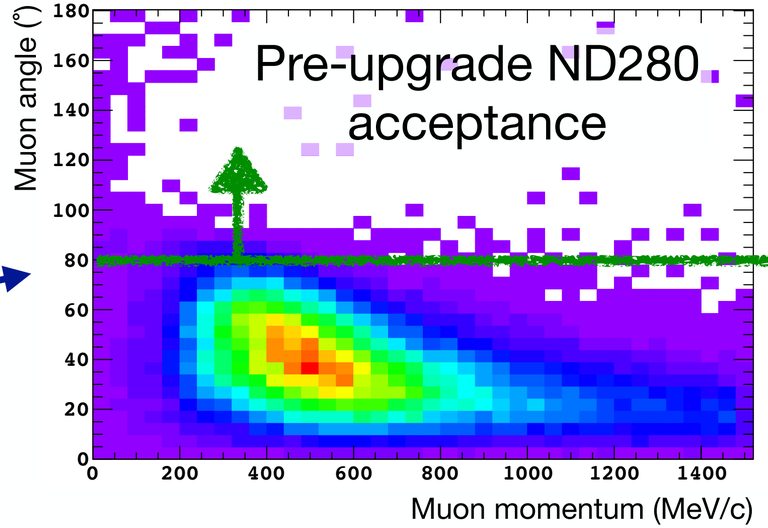

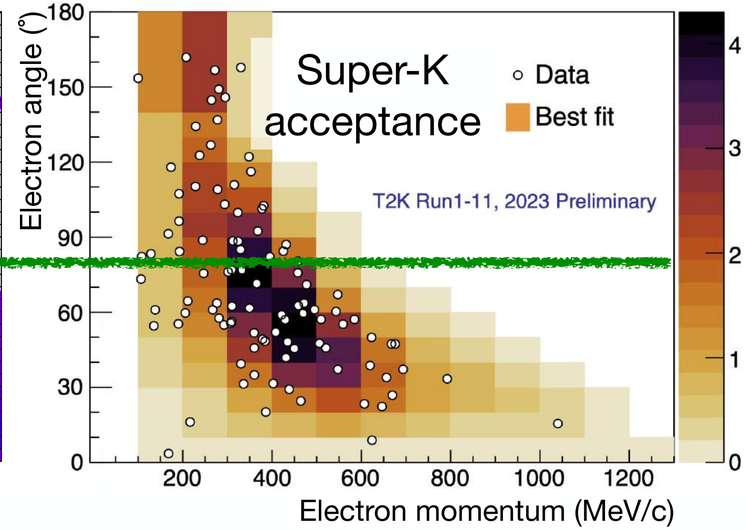

T2K Near detector upgrade

- P0D sub-detector has been replaced with:
  - a new fine grained scintillator target (Super Fine Grained Detector aka SFGD) for good low energy proton and neutron(!) reconstruction
  - two high angle TPCs (HATs) to increase the angular acceptance closer to that of Super-K
  - six time-of-flight (ToF) detector panels for directionality info of charged tracks and for veto
- Installation at J-PARC completed in May 2024

SuperFGD Design:

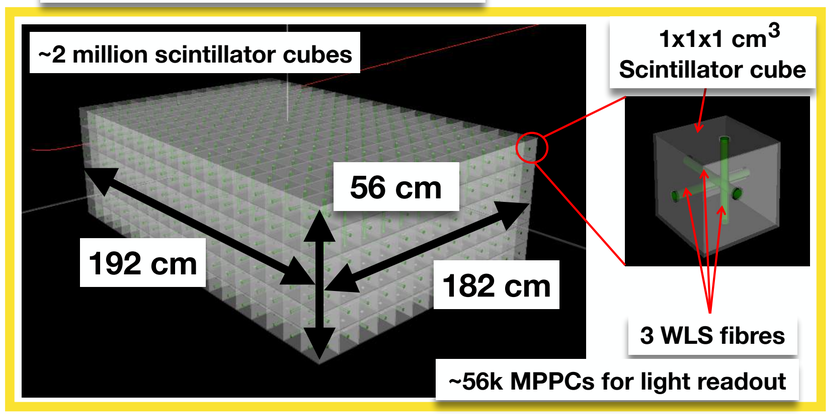

2 HTPCs Design:

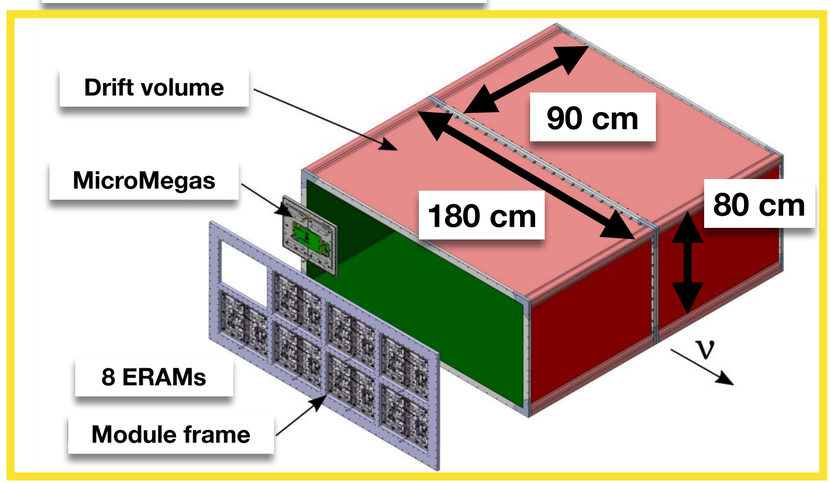

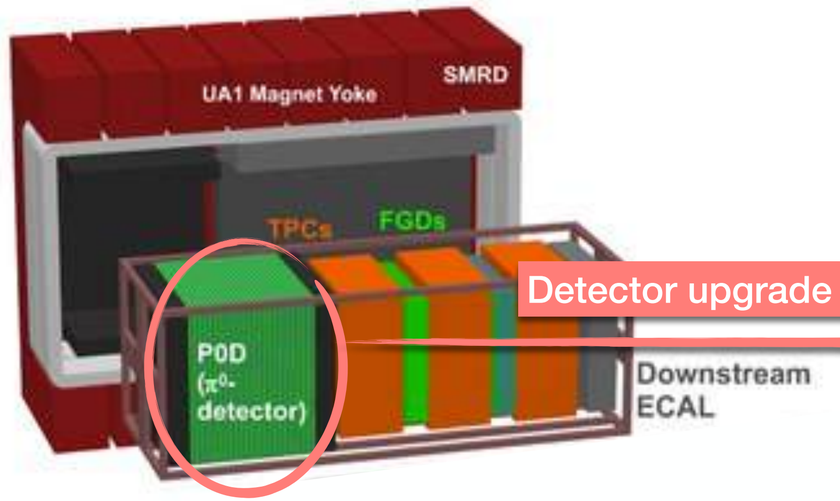

Original ND280 detector (2010-2023)

Detector upgrade in 2023/24

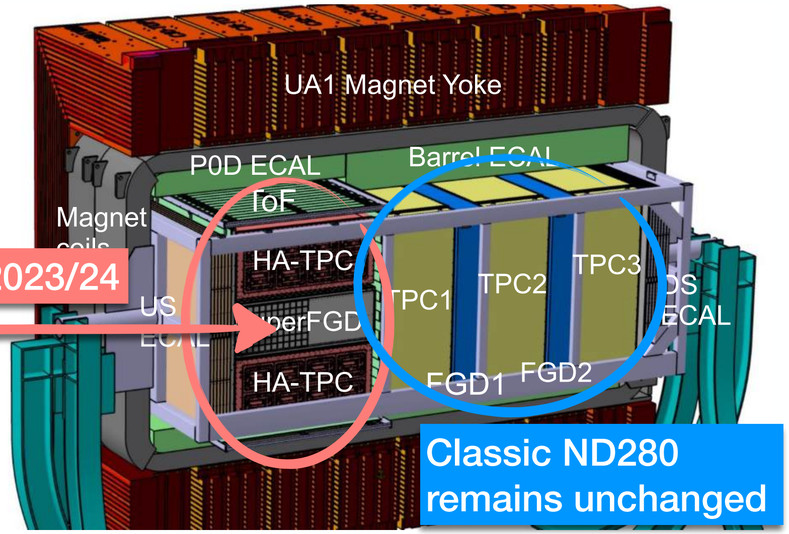

New ND280 detector (Completed in 2024)

For more details on the design, refer to the ND280 Upgrade Technical Design Report: arXiv:1901.03750

T2K Near detector upgrade

- P0D sub-detector has been replaced with:
  - a new fine grained scintillator target (Super Fine Grained Detector aka SFGD) for good low energy proton and neutron(!) reconstruction
  - two high angle TPCs (HATs) to increase the angular acceptance closer to that of Super-K
  - six time-of-flight (ToF) detector panels for directionality info of charged tracks and for veto
- Installation at J-PARC completed in May 2024

SuperFGD Design:

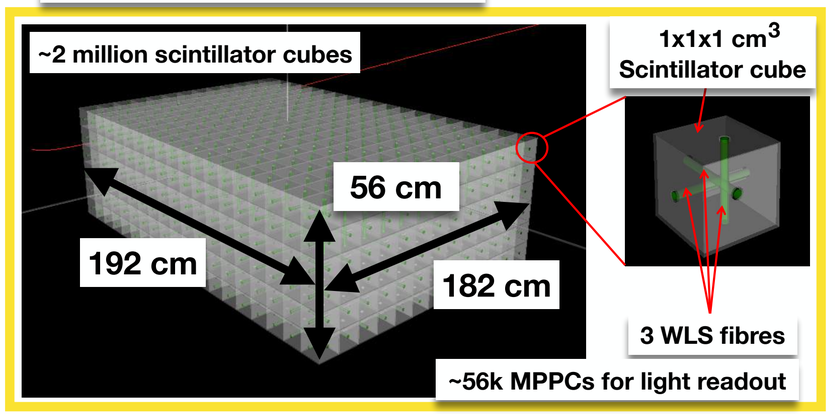

2 HTPCs Design:

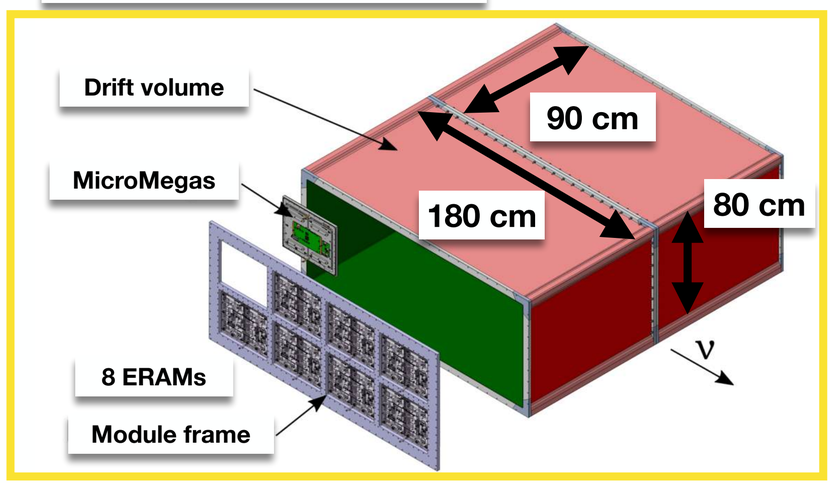

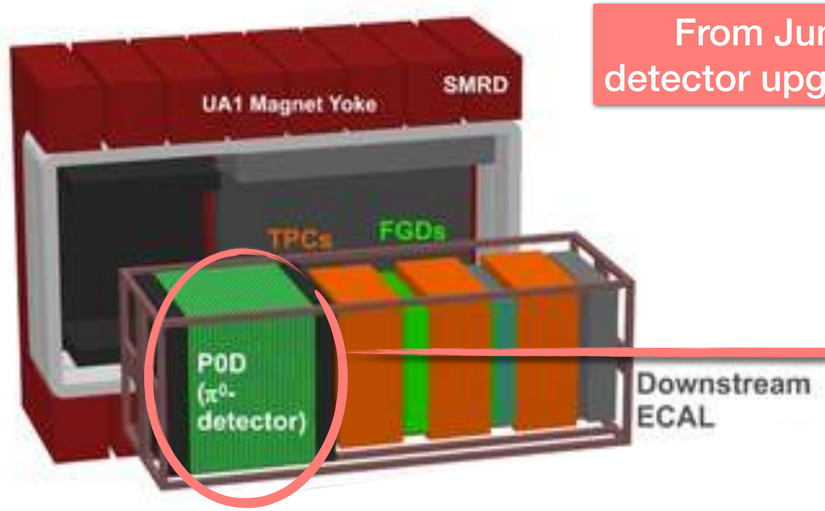

From June 2024 onwards: detector upgrade fully completed!

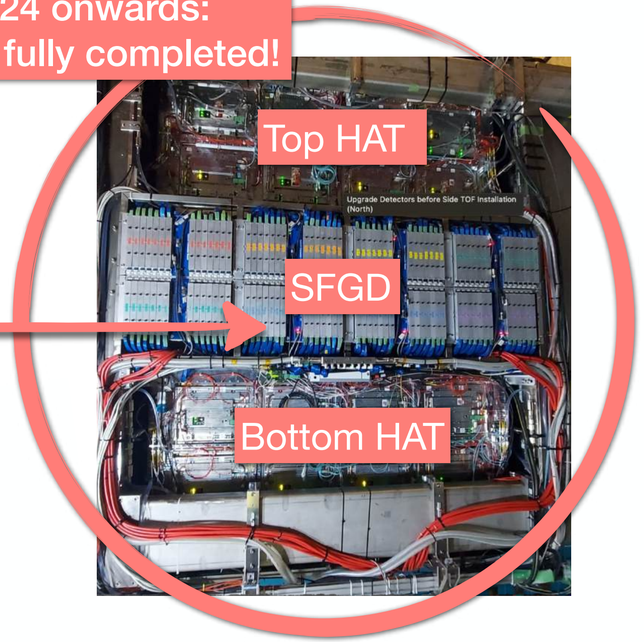

Original ND280 detector (2010-2023)

For more details on the design, refer to the ND280 Upgrade Technical Design Report: arXiv:1901.03750

SFGD scintillator cubes

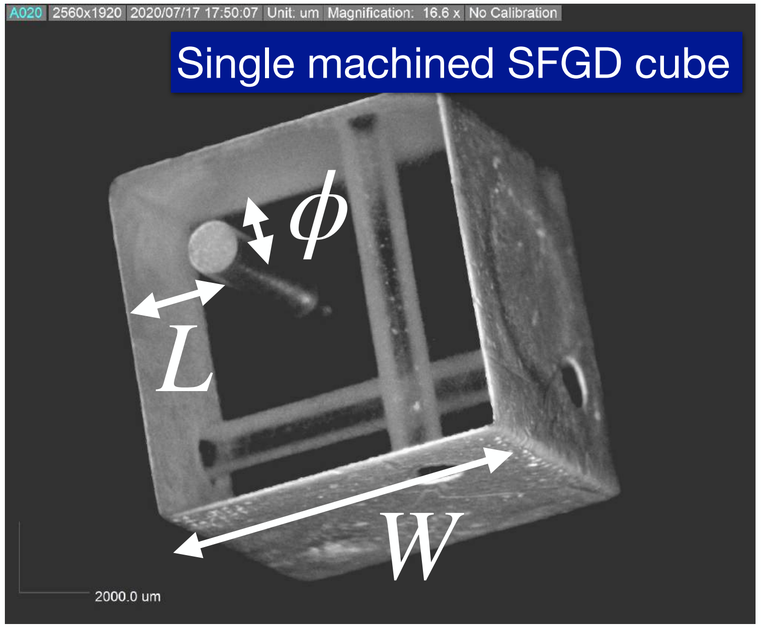

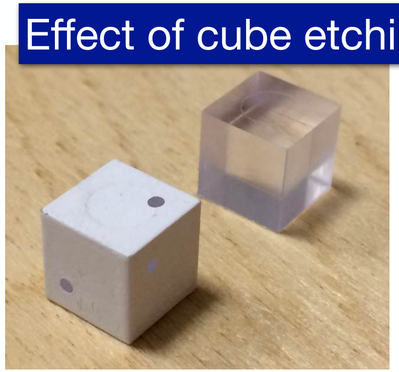

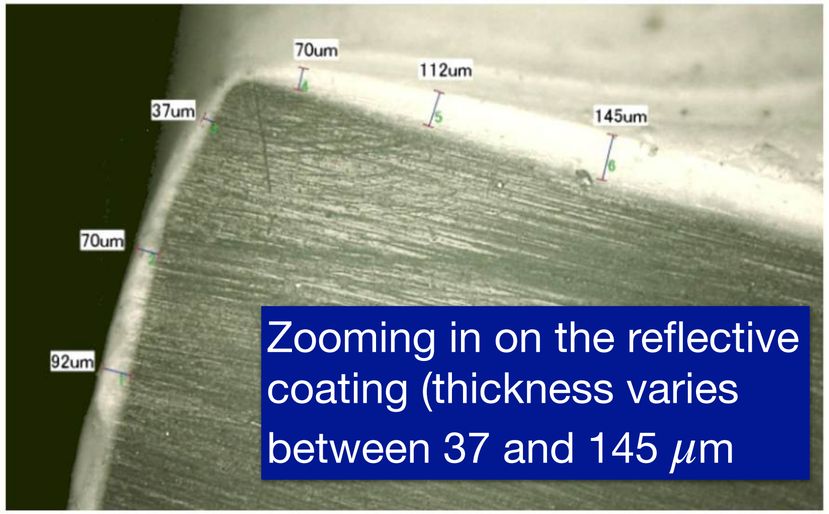

- Single SFGD cube - polystyrene with 1.5% paraterphenyl (PTP) and 0.01% POPOP, produced by the UNIPLAST Co. (Vladimir, Russia) by injection moulding (4,000 cubes per day during production process)
- Channels drilled into the cubes for optical fibre feed-through (12,000 holes drilled per day to keep up with manufacturing rate)
- Up to 5 drilling machines and 13 operators used at full production rate
- Reflective layer introduced by chemical etching the cubes (micro-porosity makes the surface appear white)
- Dimensions after etching:

$L = (2.88 \pm 41)$ mm, $W = (10.16 \pm 0.06)$ mm

($\phi \sim 1.4$ mm stainless steel rods used to mechanically reject cubes with badly drilled holes)

- Low tolerances for cube dimensions are crucial for detector assembly (~2,000,000 cubes)

SuperFGD assembly: cubes into layers into whole box

1. Cubes lined up on fishing lines

2. A total of 56 XY layers assembled at INR (Russia), and shipped to J-PARC (Japan)

3. Assembly of SFGD layers at J-PARC inside the mechanical box (two box sides are visible)

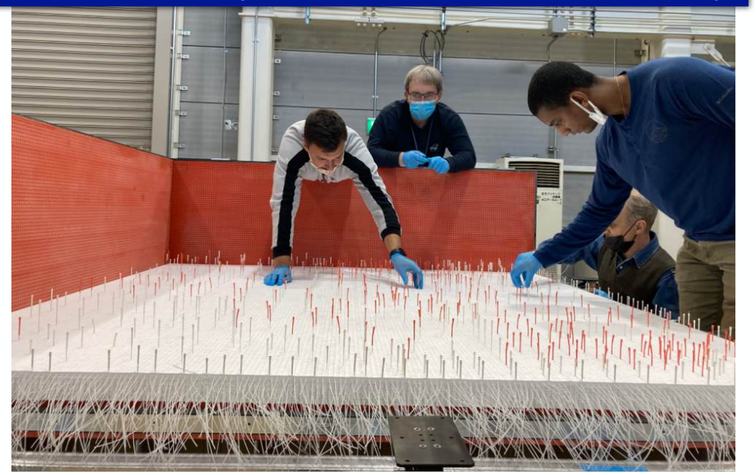

4. Completion of SFGD layers' assembly at J-PARC

5. Removal of fishing lines and installation of WLS fibres after closure of the mechanical box

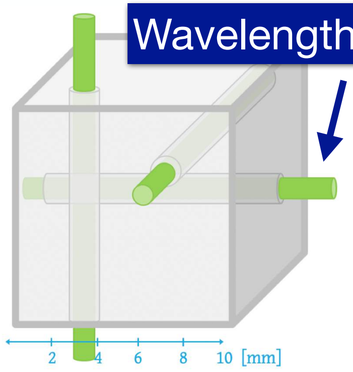

- 1,956,864 cubes (56x182x192)
- 55,888 electronics readout channels (one per WLS fibre)
- 111,776 drilled holes
- 536 kg: weight of empty mechanical box that holds equipment together

SuperFGD photosensors

Light detection principle

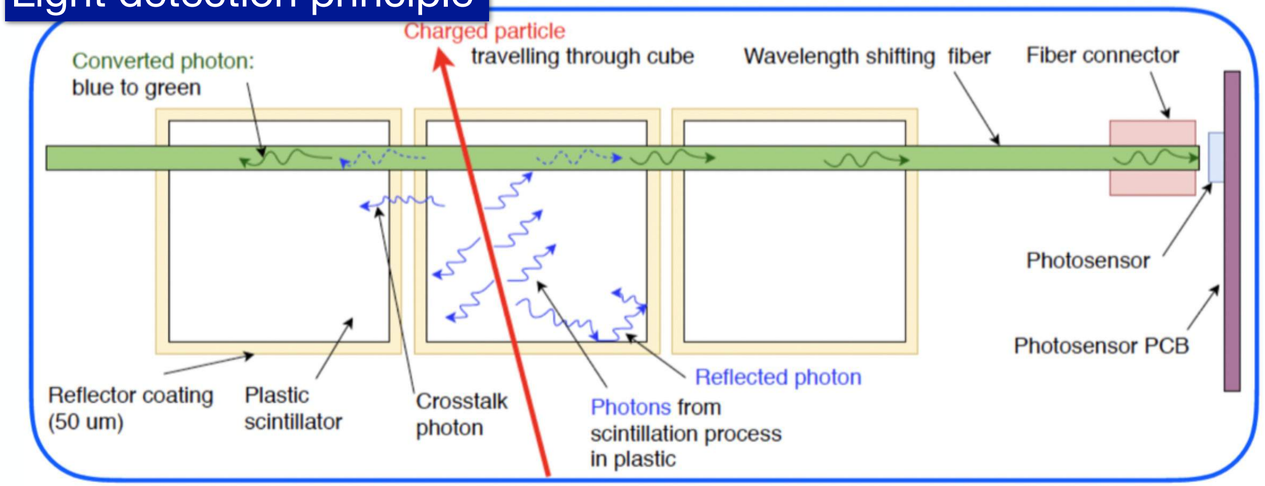

HAMAMATSU
PHOTON IS OUR BUSINESS

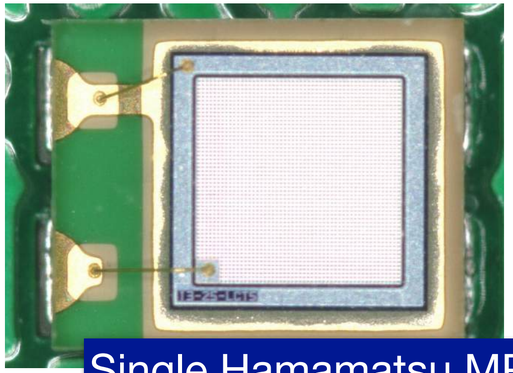

Single Hamamatsu MPPC (S13360-1325PE)

- Wavelength-shifting fibres carrying the light: Y-11 (Kuraray Co.) of ϕ 1.0 mm
- Horizontal fibres ~2 m length, vertical fibres ~60 cm

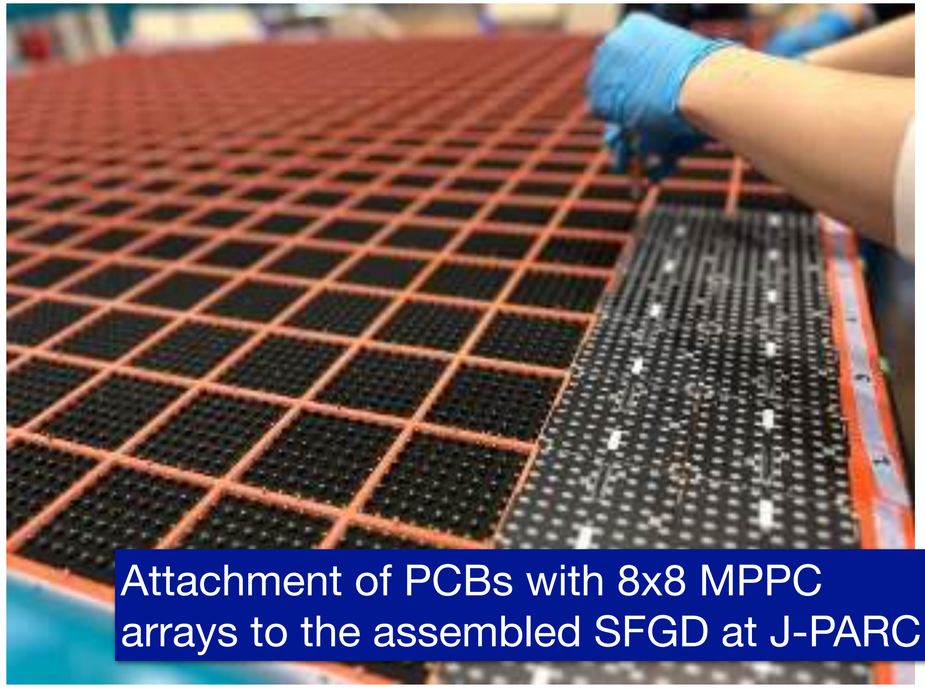

Attachment of PCBs with 8x8 MPPC arrays to the assembled SFGD at J-PARC

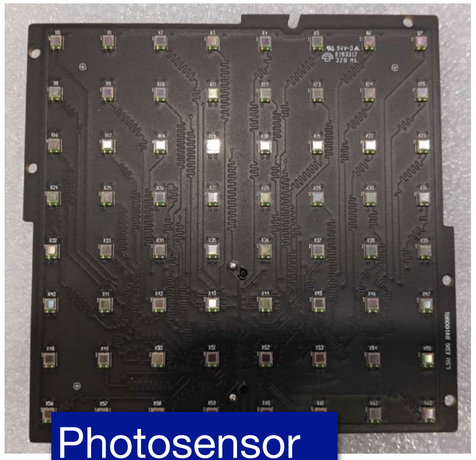

Photosensor side of PCBs

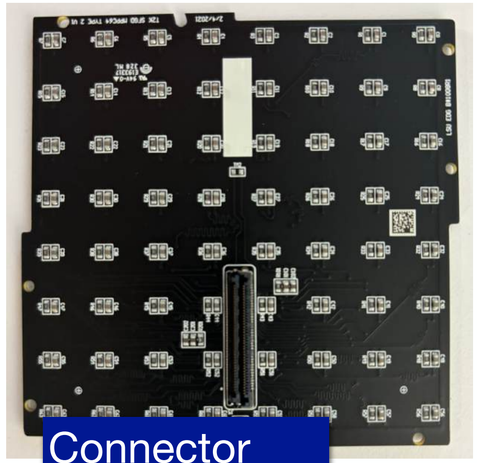

Connector side of PCBs

Item	Specification
Effective photosensitive area	1.3 mm x 1.3 mm
Pixel pitch	25 μm
Number of pixels	2668 pixels
Fill factor	47%
Package type	Surface mount
Breakdown voltage (V_{BR})	53 $\pm$ 5 V
Peak sensitivity wavelength	450 nm
Photo detection efficiency	25%
Gain	7.0 x 10^5
Dark count	70 kcps (typ.)
Crosstalk probability	1%

SuperFGD LED calibration system

Operation principle of the LED calibration system

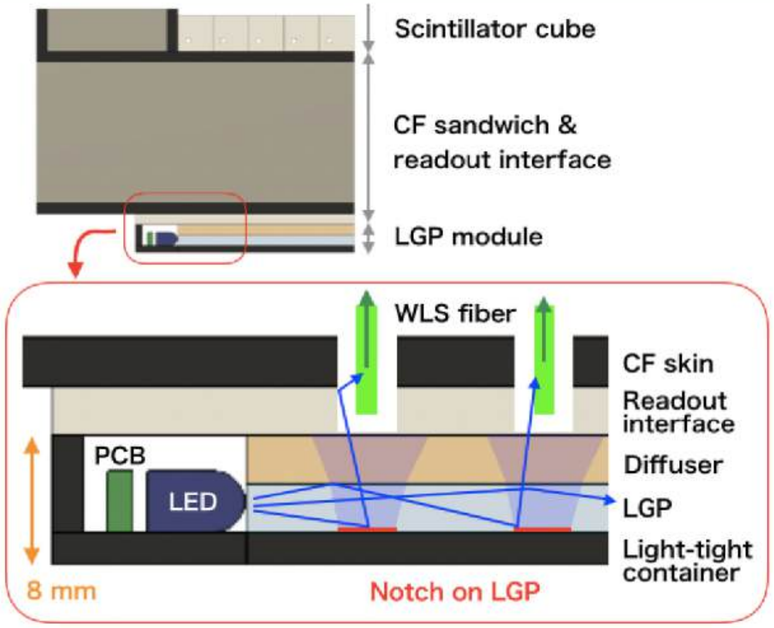

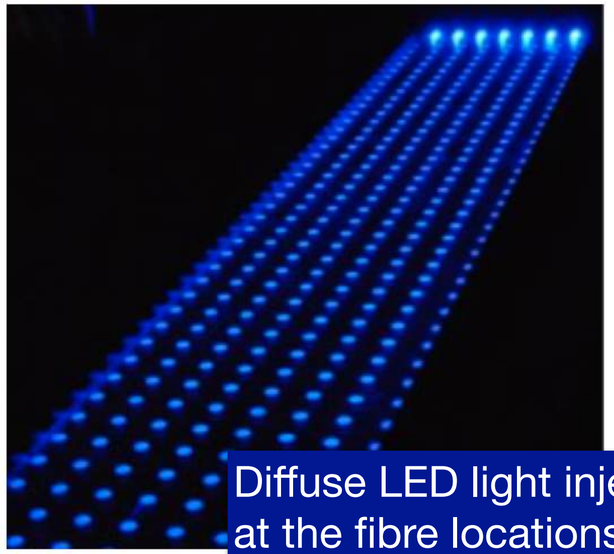

Diffuse LED light injected at the fibre locations

- LED system has been deployed to monitor detector stability and performance and to perform gain calibration
- LED system is attached to the WLS fibres on the other end from the MPPC readout side
- A combination of a Light-Guide-Plate (LGP) and the Diffuser carries LED light to the fibres uniformly

LGP module design

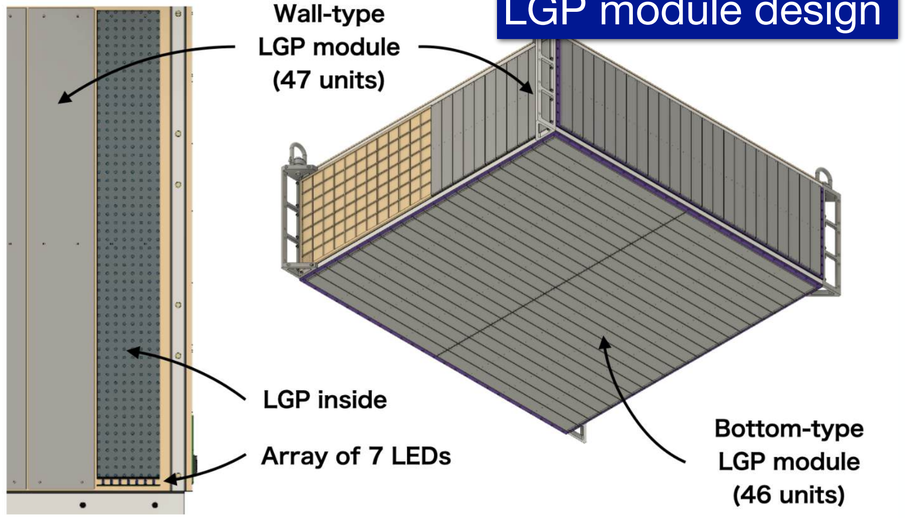

LGP modules of the “wall-type” installed at the downstream end of the fully assembled SFGD

SuperFGD DAQ design and performance

- October 2023: SFGD detector assembly completed
- Commissioning of the DAQ system was first performed stage-wise (with ~20% and ~50% FEBs) on the surface, before installation in the ND280 pit
- Beam operation in November/December 2024 was with ~80% FEBs (~50,000 readout channels)
- Full electronics installation in the pit completed in March 2024 and tested during the summer 2024 data collection

One vertical side of SFGD showing the fully installed readout electronics

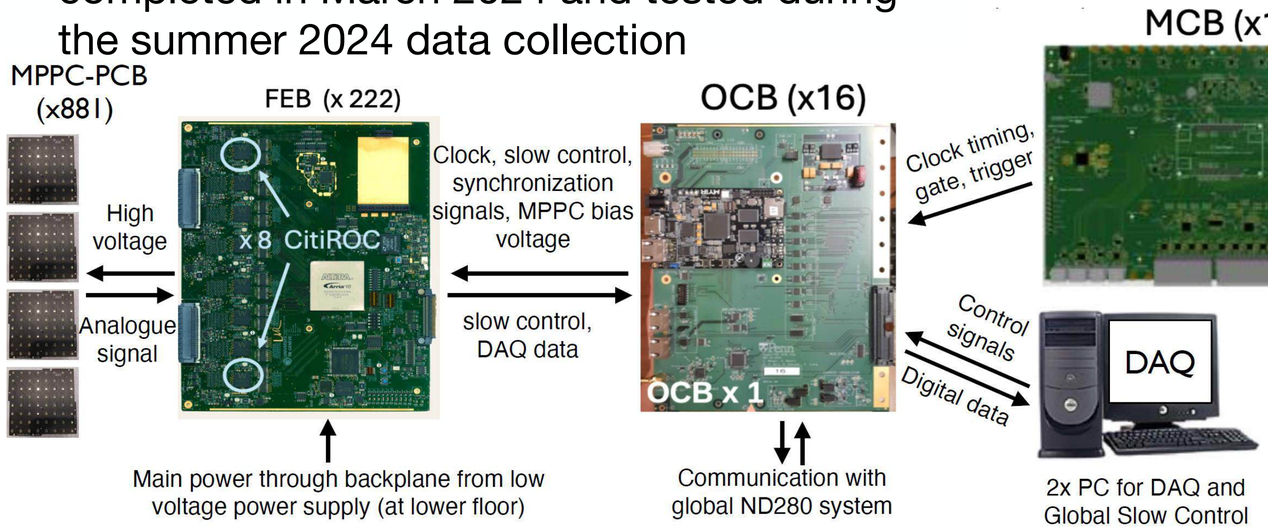

Data taking efficiency of SFGD achieved during the June 2024 run was over 99% (and 96.1% for the entire ND280)!

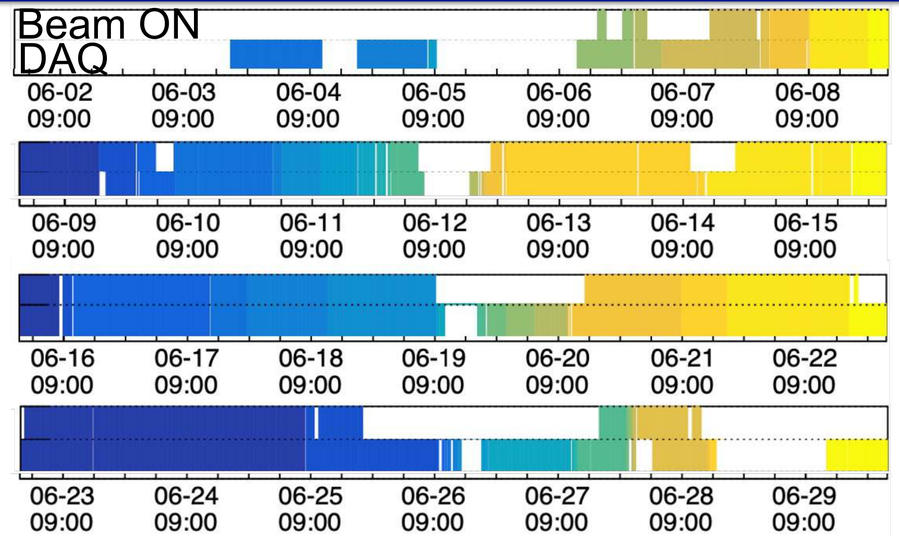

SuperFGD prototype at CERN

CERN SFGD Prototype

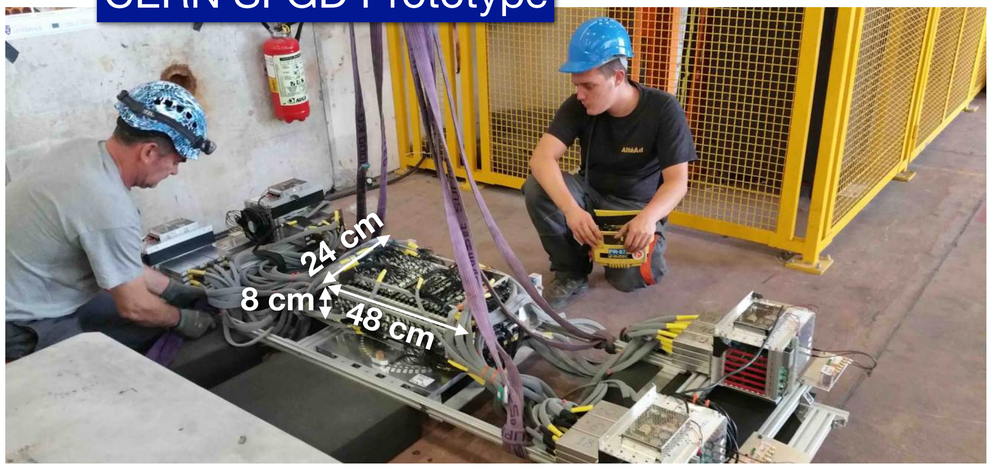

- CERN prototype commissioning and detector performance characterisation with charged particle beams: *JINST 15 (2020) 12, P12003*
- Also LANL prototype commissioning (2019-2020) to quantify capacity to measure neutron kinematics: *Phys. Lett. B 840 (2023) 137843* (more on this later)

CERN Prototype placed in the test beamline

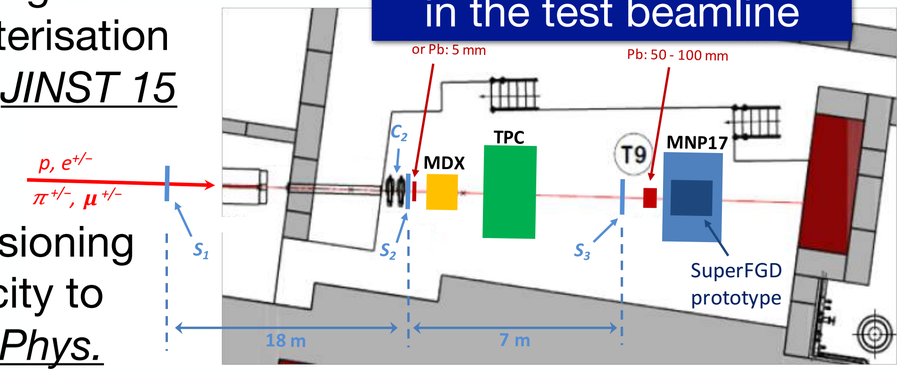

Excellent separation between protons and MIP-like particles based on energy loss (here shown at fixed 0.8 GeV/c beam momentum, 0.2 T magnetic field)

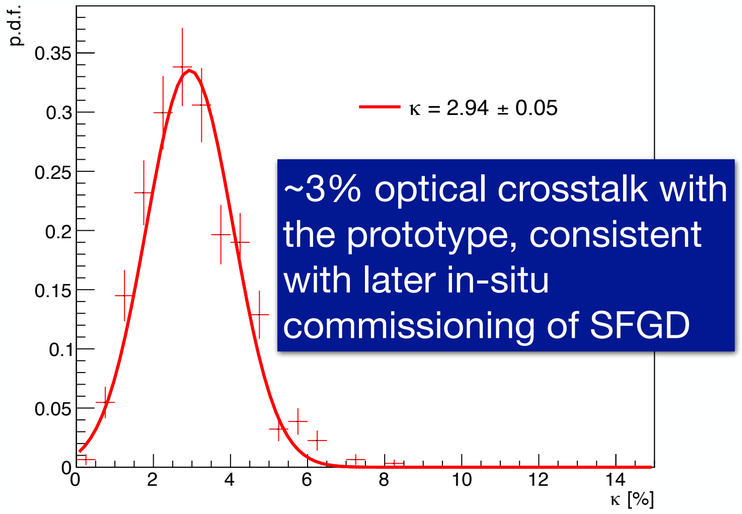

~3% optical crosstalk with the prototype, consistent with later in-situ commissioning of SFGD

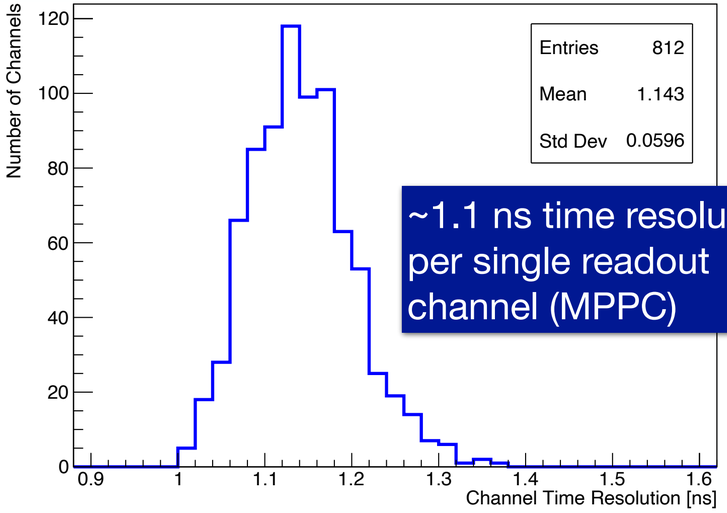

~1.1 ns time resolution per single readout channel (MPPC)

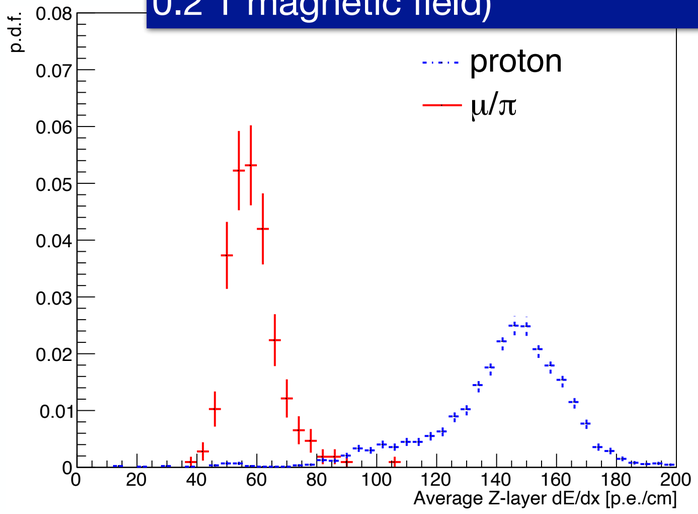

SFGD preliminary performance at J-PARC: readout electronics

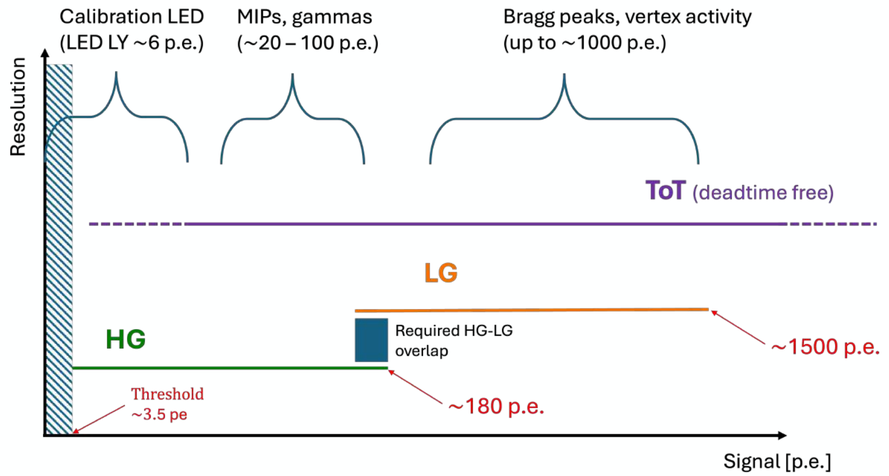

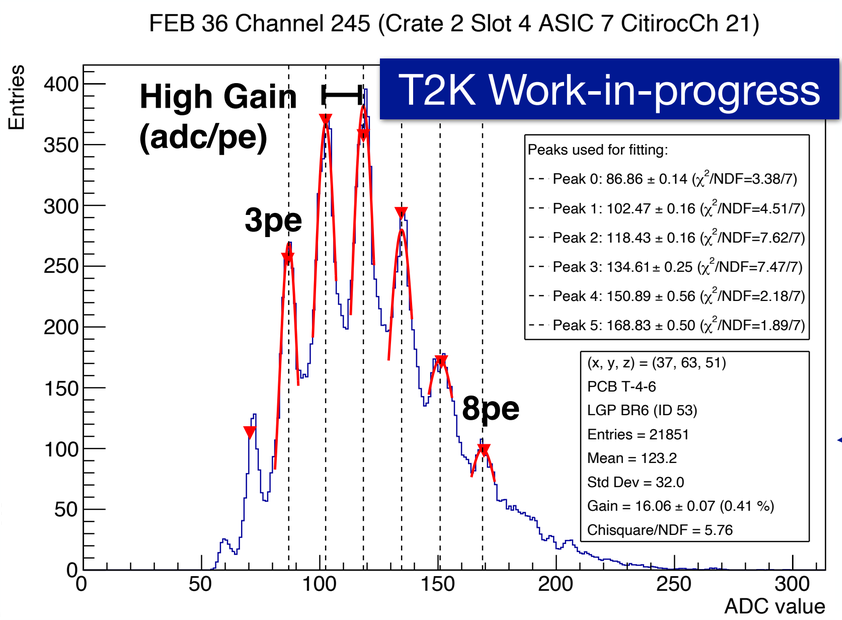

Example of how the single channel gain is quantified by fitting p.e. peaks to the measured ADC distribution for a single channel at a fixed voltage setting

- Readout electronics covers a wide dynamic range ~3.5 to ~2,000 p.e.
- MPPC gains (in high and low voltage settings) are calibrated and their stability monitored both during data acquisition (by shining the LED between neutrin beam spills) and on maintenance days
- For every MPPC, the gain (ADC value per 1 p.e.) is found by fitting p.e. peaks to the measured LED induced distribution
- The gain pedestal is quantified from LED data collected at different voltage settings
- Both the channel pedestal and gain are highly stable during data taking (e.g. in normal conditions mean gain fluctuates by <0.5%)

Pedestal stability

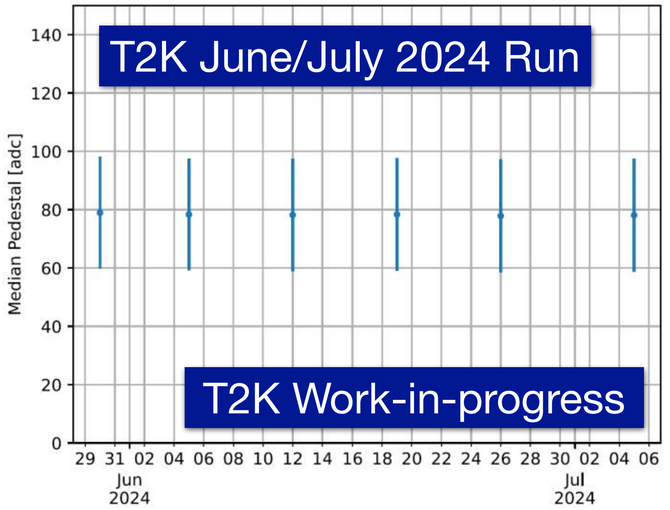

MPPC gain stability

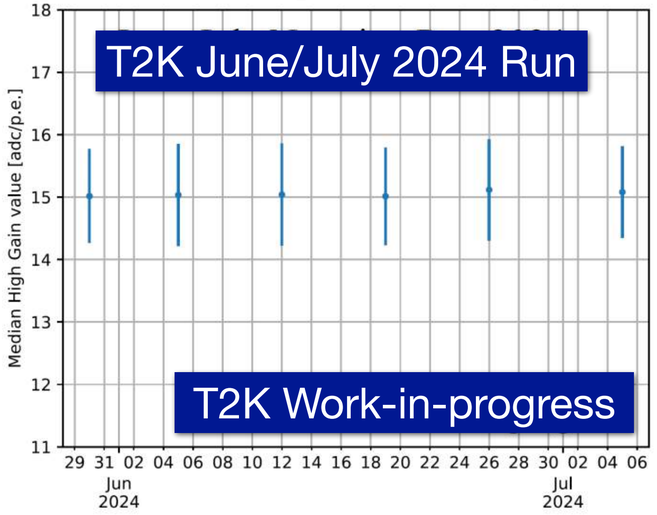

SFGD preliminary detector performance at J-PARC

- Preliminary detector performance is showing good results: post-calibration timing resolution and channel crosstalk are consistent with prototype commissioning, light attenuation is consistent with fibre properties, stopping particle features such as Bragg peak are visible

- First physics analyses of the data sets collected with the upgraded detector are in progress

Optical crosstalk between scintillator cubes

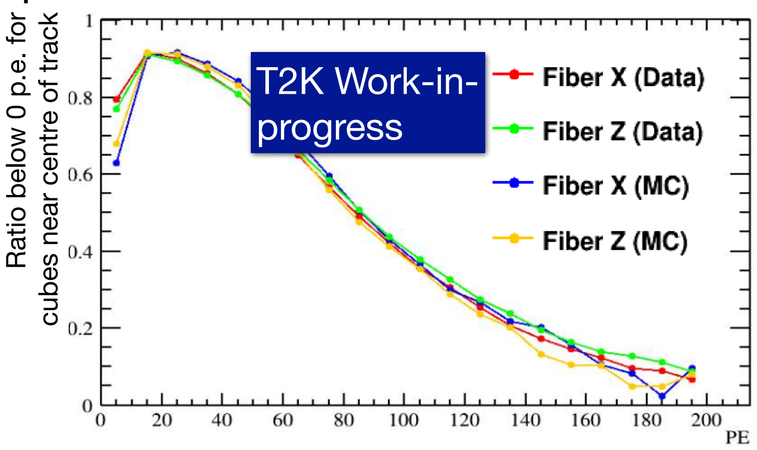

Best agreement with data found when simulating ~3% MC crosstalk

Light yield and attenuation in fiber

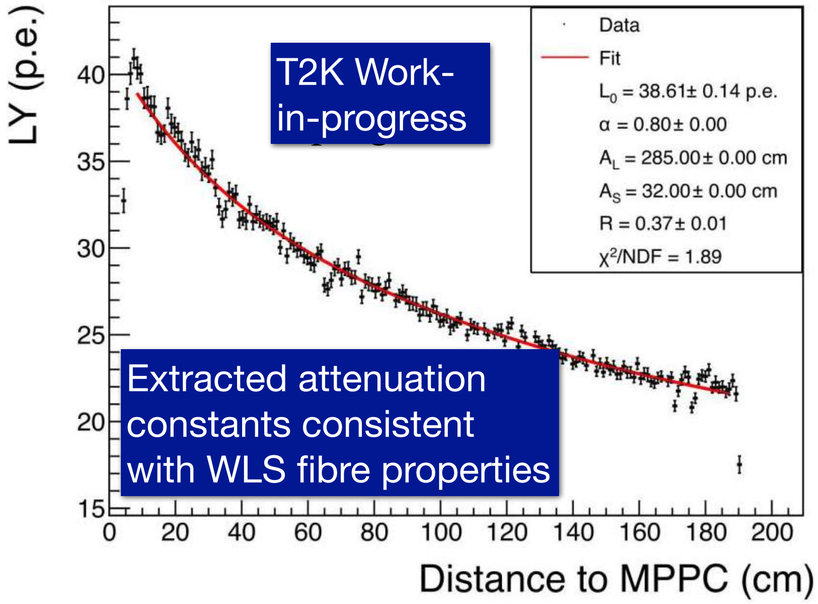

Time resolution

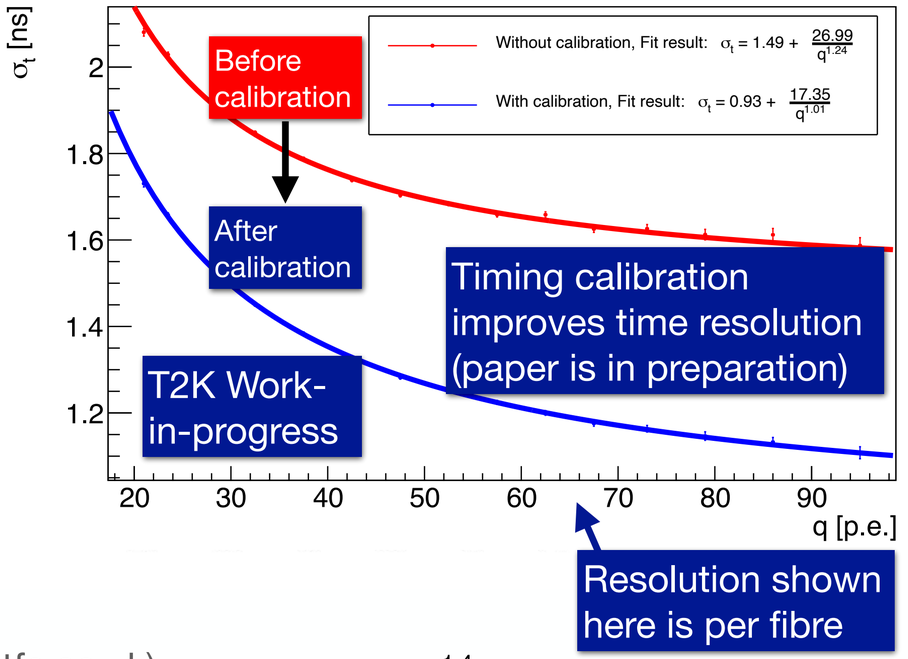

Stopping proton analysis

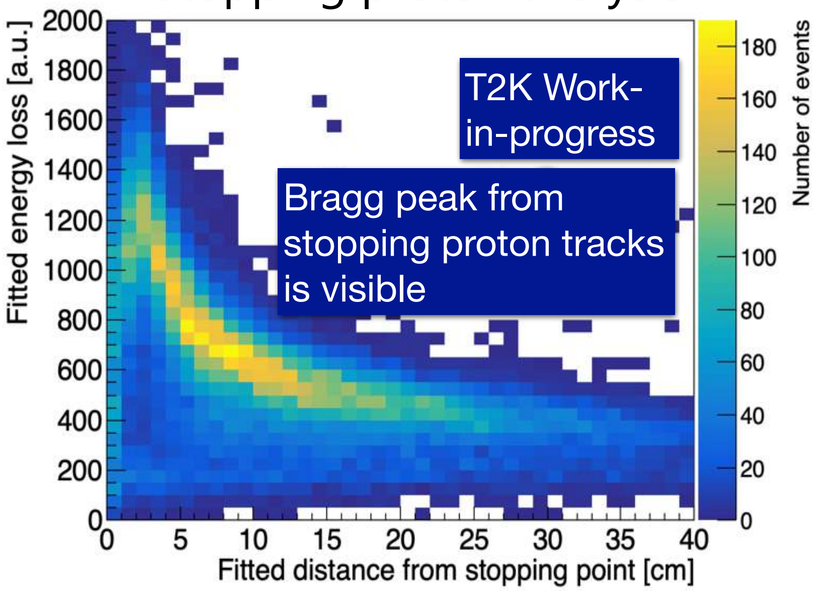

Examples of event displays with the upgraded detector

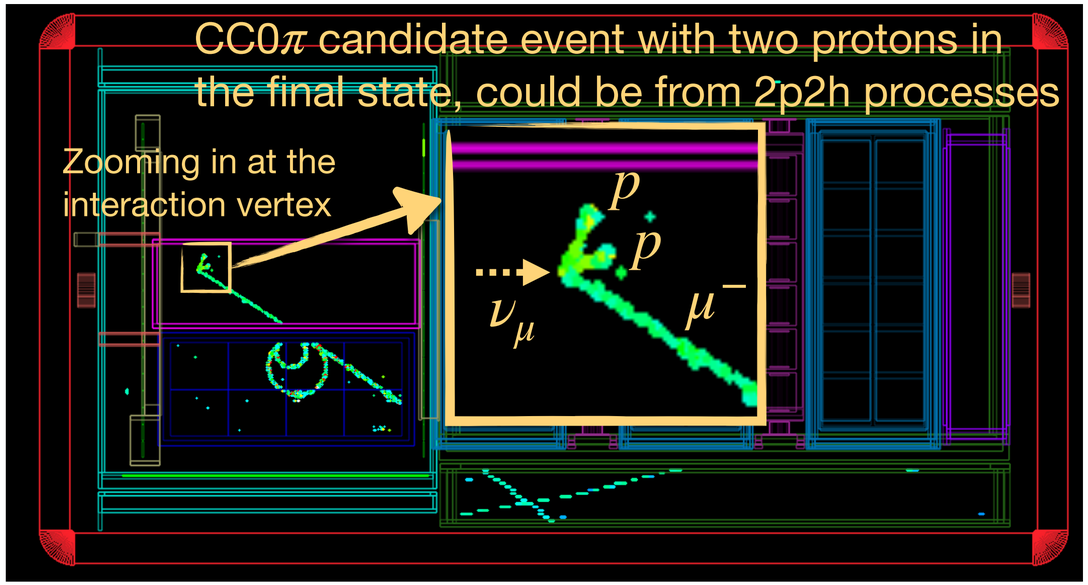

- Unprecedented resolution around the interaction vertex and level of detail for the T2K near detector has been achieved during commissioning of the upgraded ND280 with the T2K beam
- Shown here are few of the events from the June/July 2024 T2K run

Hit Times From Beam Data, 8 June 2024

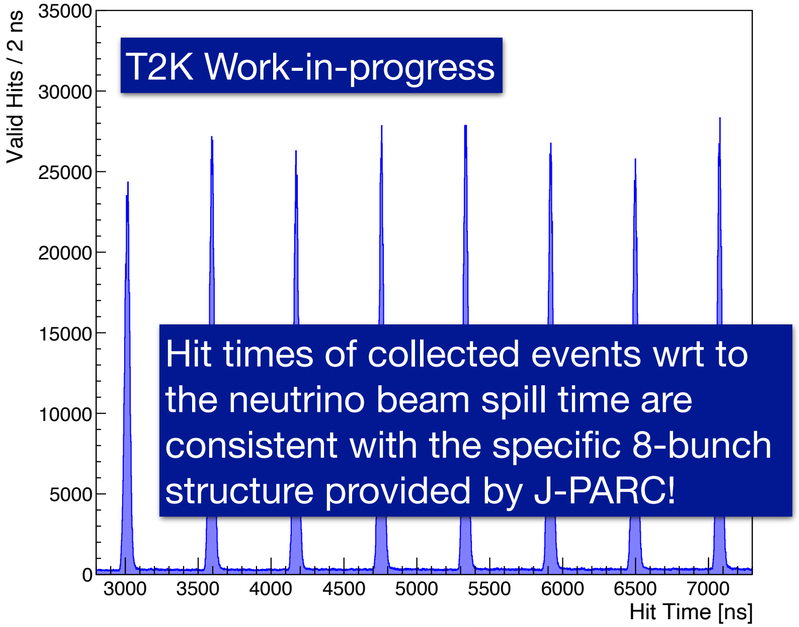

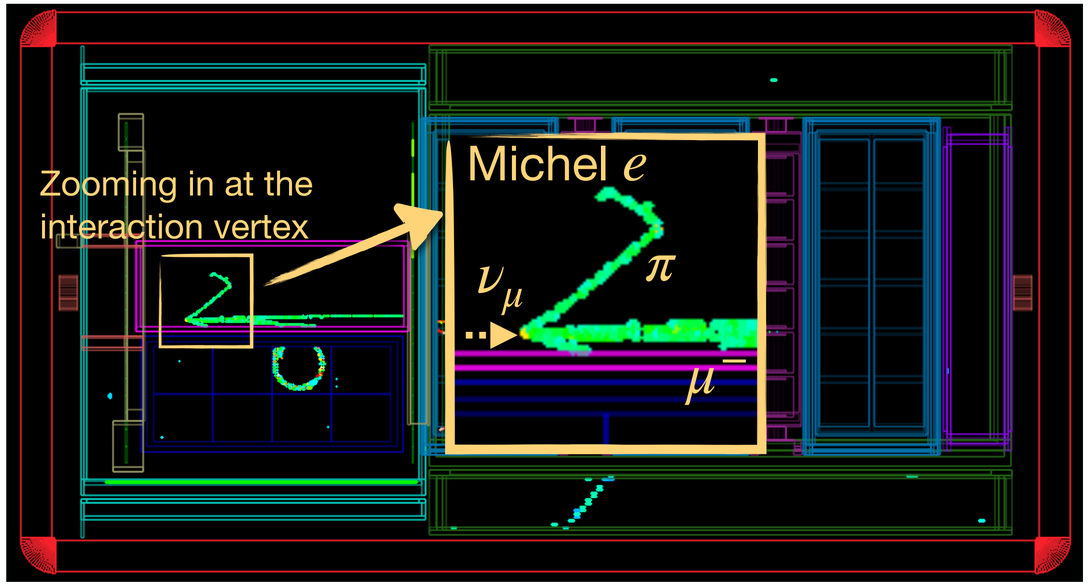

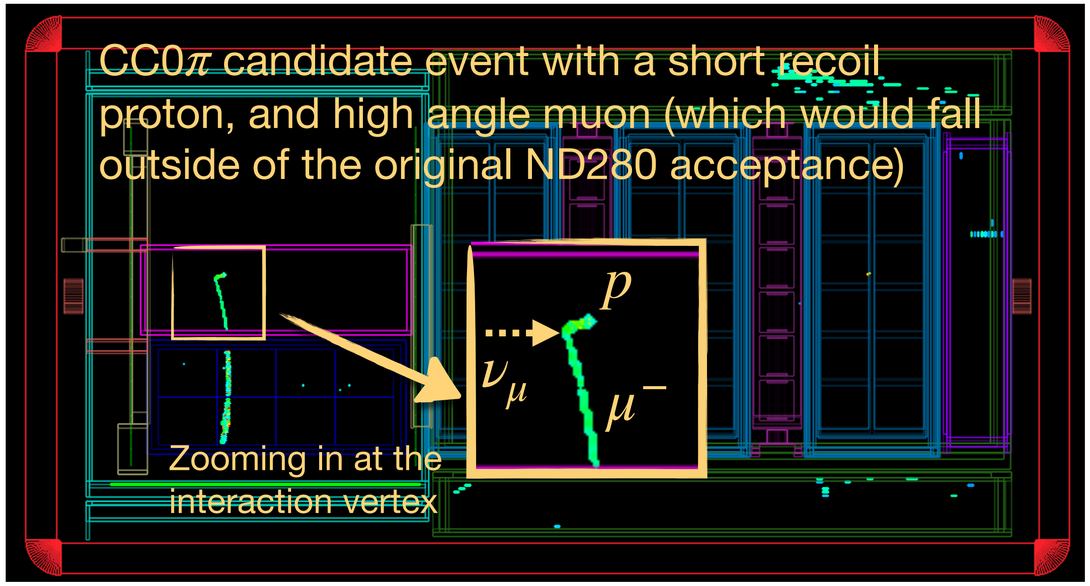

Proton threshold reduction and improved purity

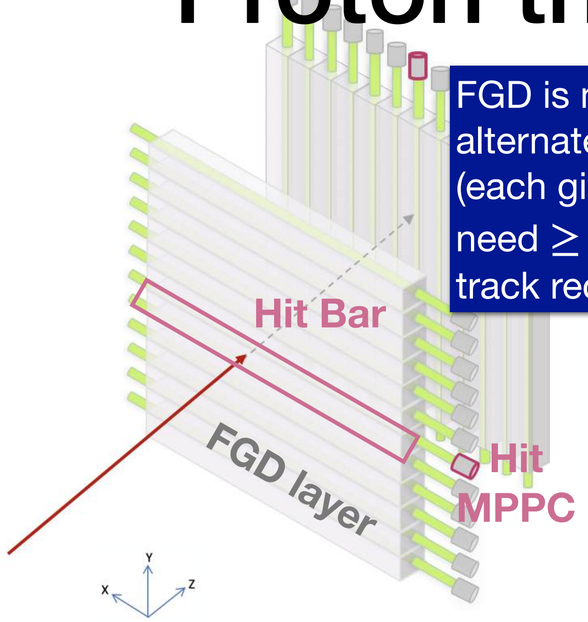

FGD is made of alternately oriented bars (each gives 2D info): need $\geq$ 4 cm tracks for track reconstruction

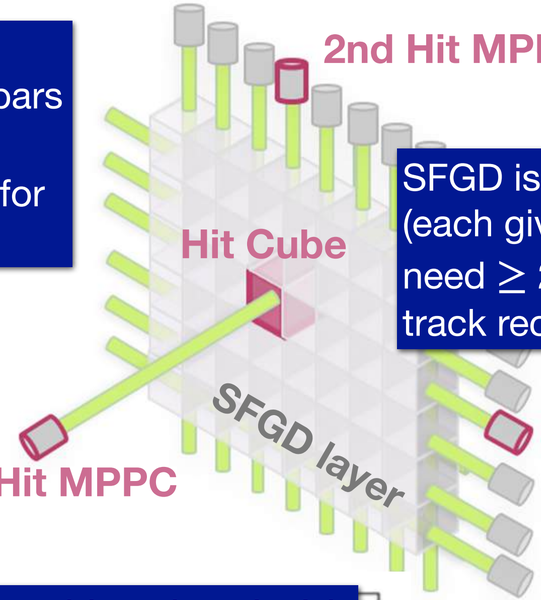

SFGD is made of cubes (each gives 3D info): need $\geq$ 2 cm tracks for track reconstruction

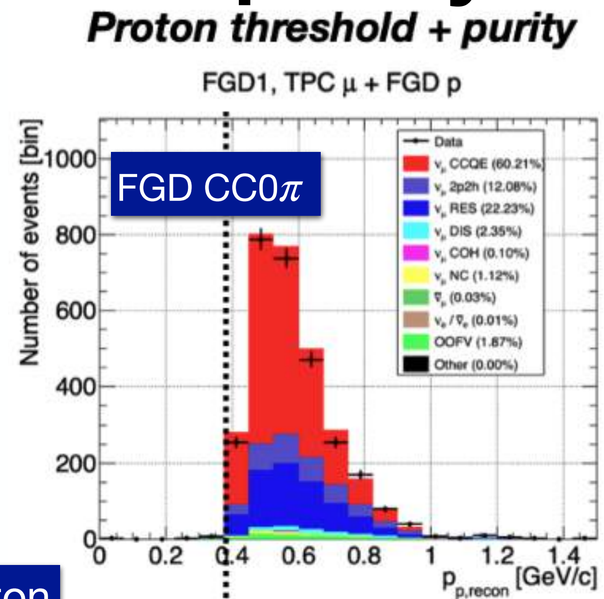

Lower proton threshold
Better CCQE purity

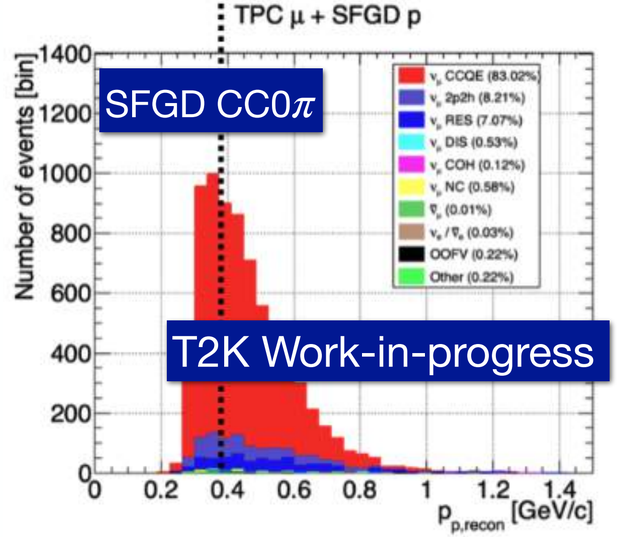

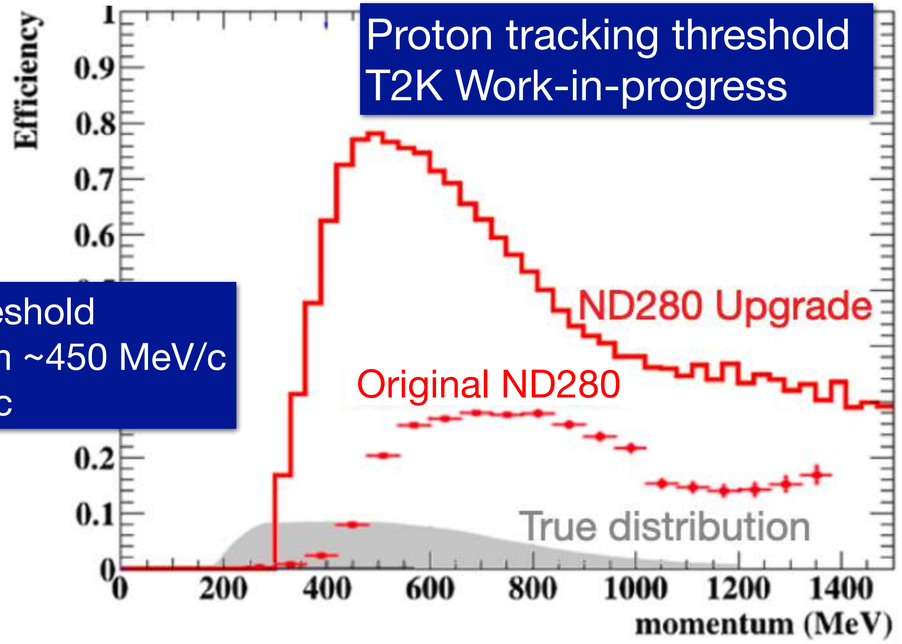

Tracking threshold reduced from ~450 MeV/c to 300 MeV/c

One of the SFGD multi-proton CC0π candidate events

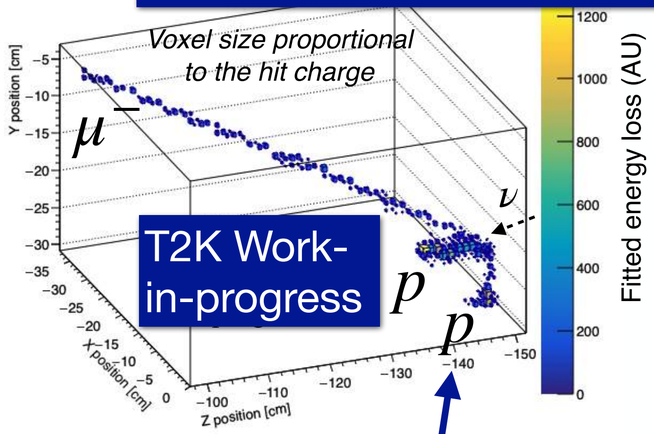

Proton multiplicity around vertex is better resolved

Neutron detection with SFGD

- For the first time, neutron reconstruction will be possible, by identifying time of flight between the $\bar{\nu}$ interaction vertex and secondary vertex of the pre-thermalisation re-interaction of the outgoing neutron (50% tagging efficiency)
- The impact that this neutron detection will have on energy reconstruction of T2K anti-neutrino's has been assessed: resolution is reduced from ~15% to ~7%

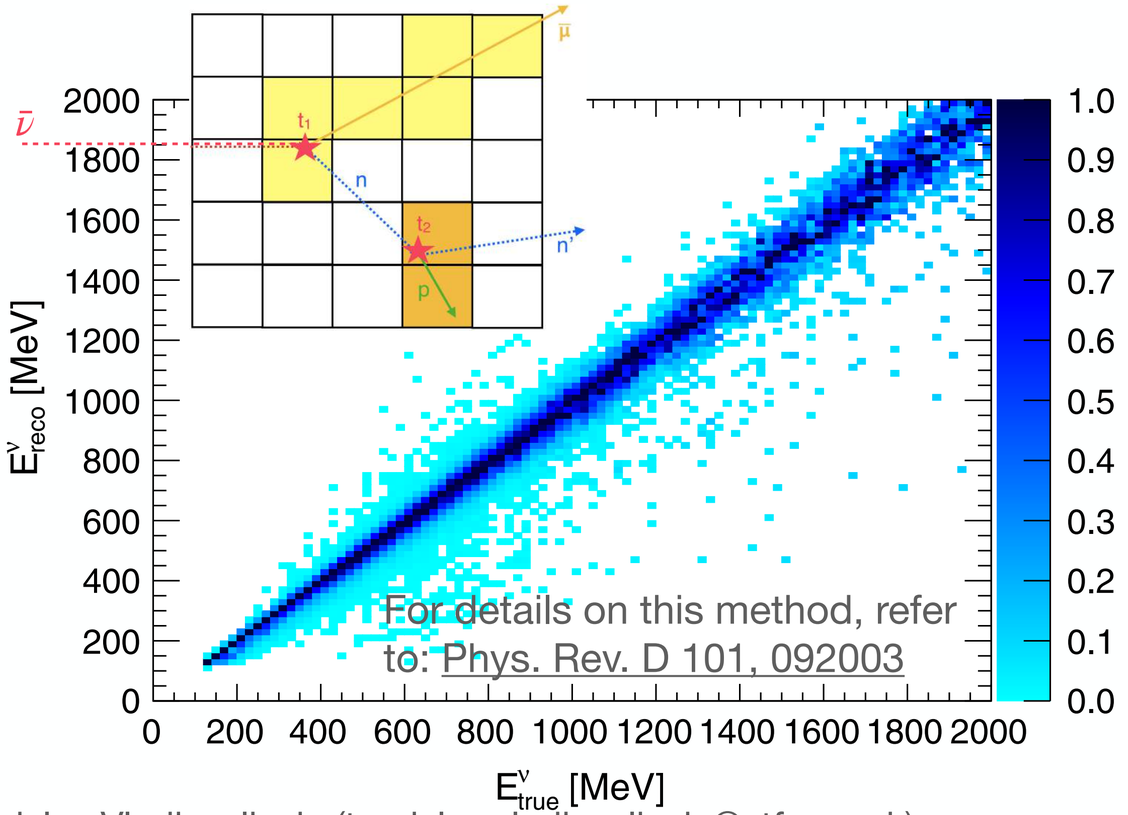

- Neutron detection has been demonstrated with the SFGD prototype exposed to the LANL neutron beamline
- For the measured total neutron cross section refer to Phys. Lett. B 840 (2023) 137843

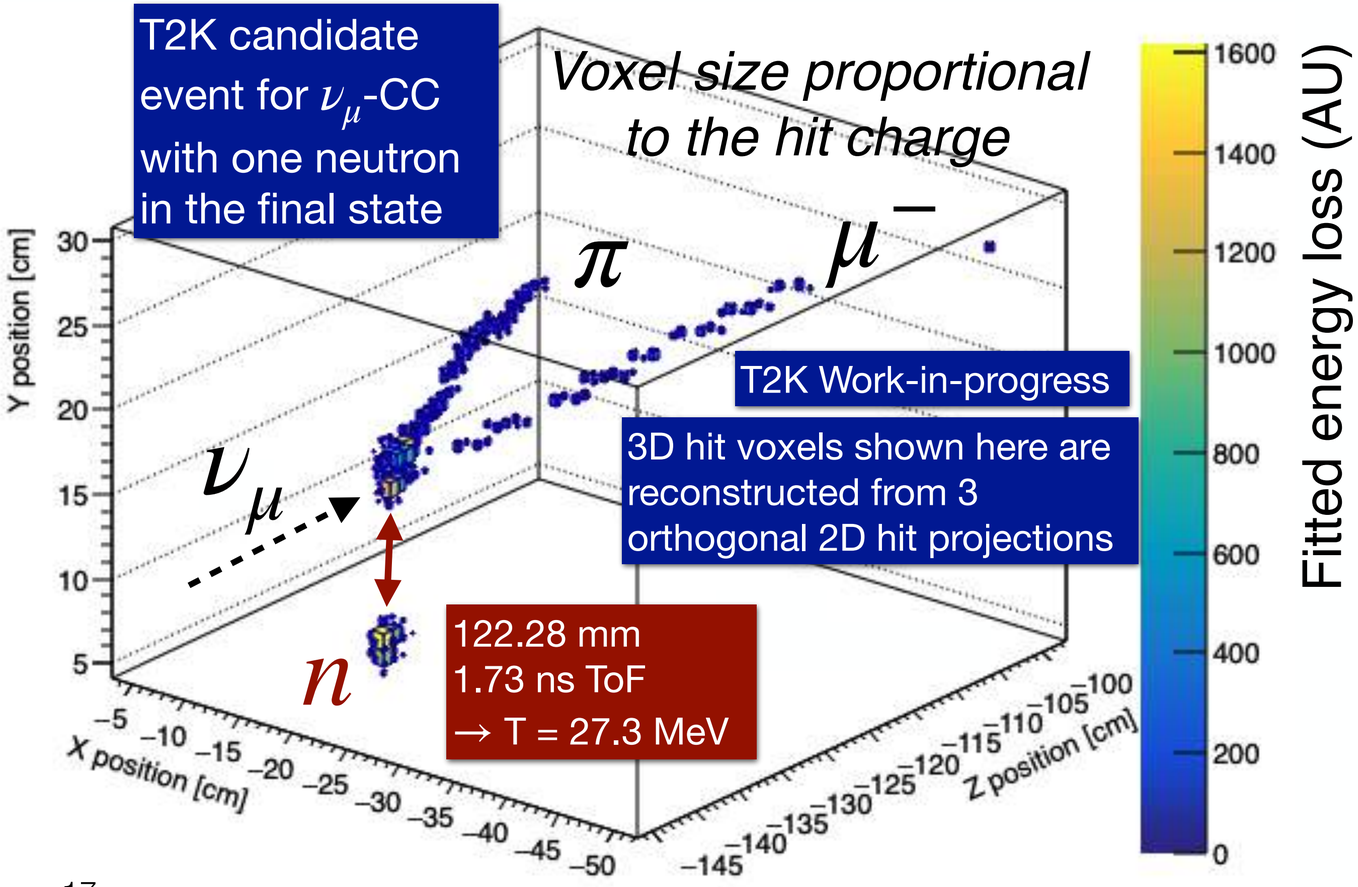

Improved ν_e selection with SFGD

- Dominant background on ν_e selection with pre-upgrade ND280 are photons from NC1Pi0
- Improved separation between single $e^{\pm}$ and $e^{\pm}$ from γ conversion enabled by the detector granularity

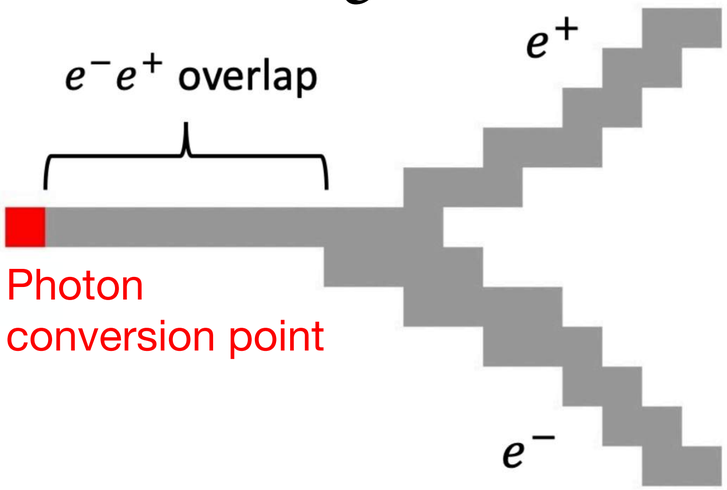

ν_e selection with original ND280

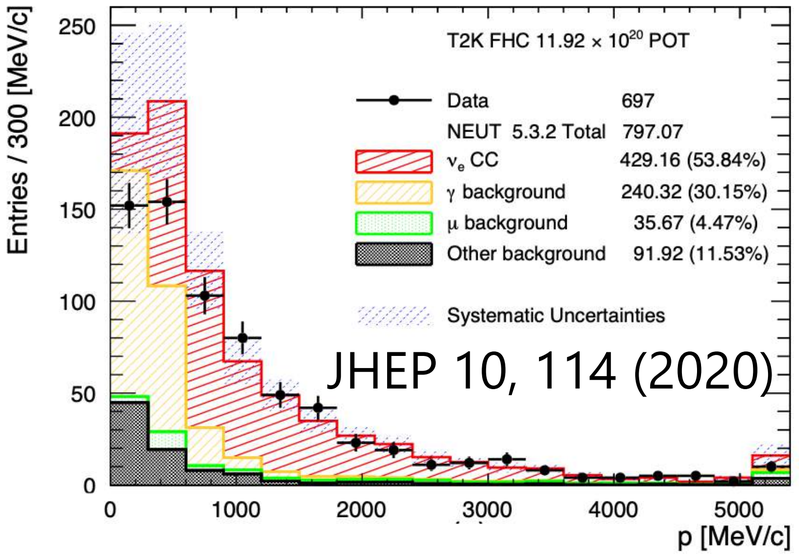

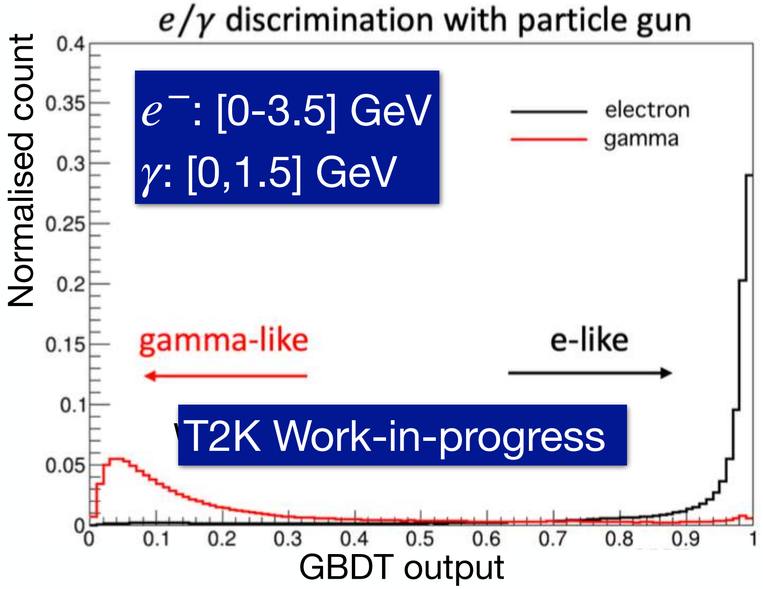

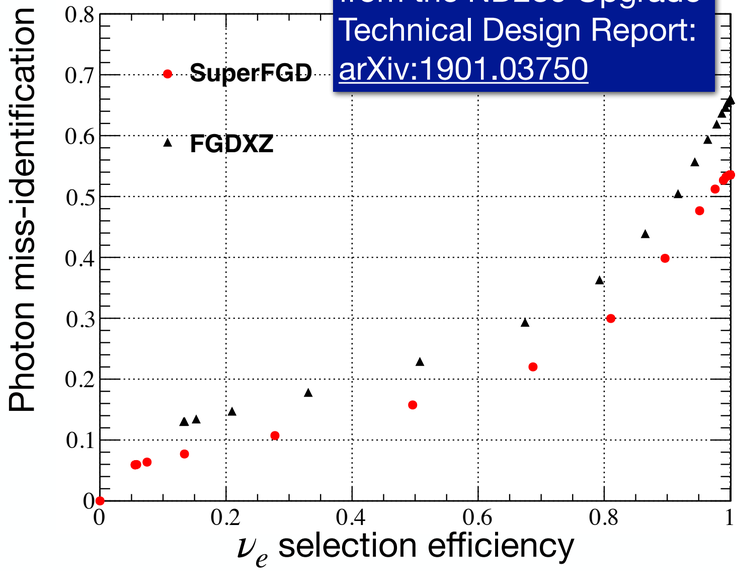

Expected performance from the ND280 Upgrade Technical Design Report: arXiv:1901.03750

ν_e selection with upgraded ND280

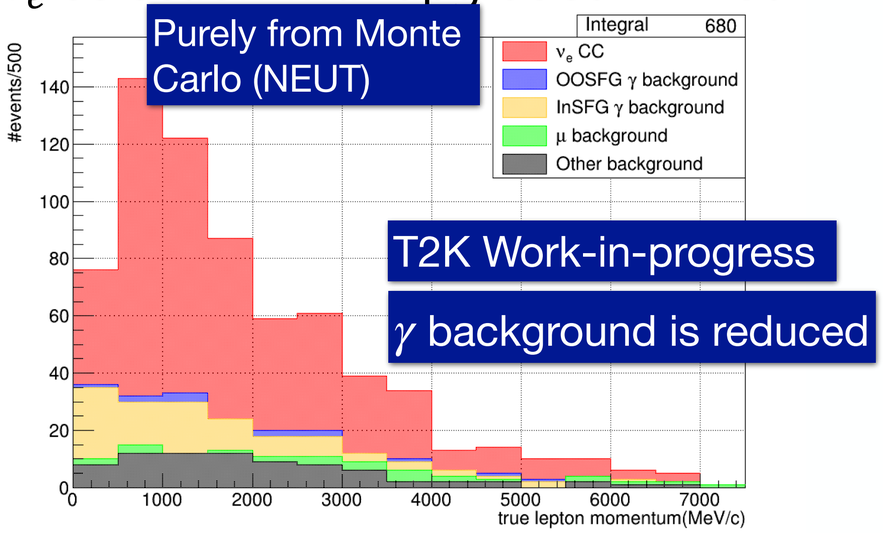

Summary

- Thanks to a huge campaign that was in making for many years, T2K ND280 upgrade is complete
- SFGD was designed, built and commissioned through a combined effort of 37 institutions from France, Germany, Japan, Russia, Switzerland, UK and USA (including CERN contribution)
- The full post-upgrade ND280 was commissioned during the June/July 2024 T2K physics run, and further runs (2.7e20 POT) were collected in November/December 2024 and March/April 2025
- The upgrade unlocks a rich physics programme and allows for numerous improvements, including faster statistics acquisition to be able to make 3σ level statements on δ_{CP}
- Data analysis is ongoing
- SFGD detector paper is in preparation
- Stay tuned for exciting new physics from T2K with the J-PARC neutrino beam

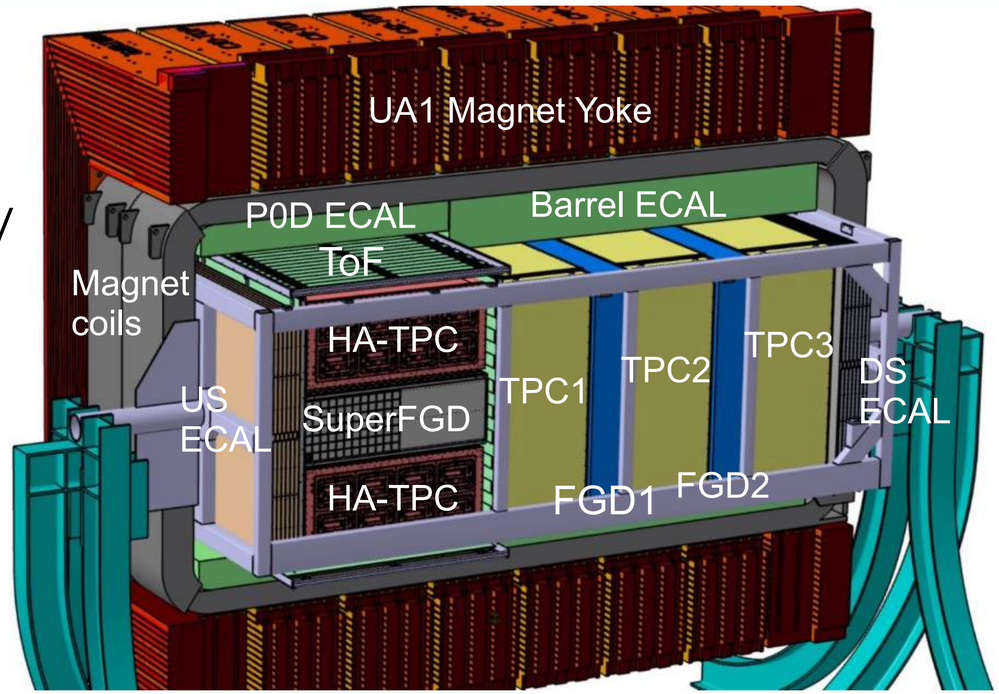

Event number : 345342 | Run number : 16847 | Spill : 28852 | Time : Fri 2024-06-07 18:29:00 JST |Trigger: Beam Spill

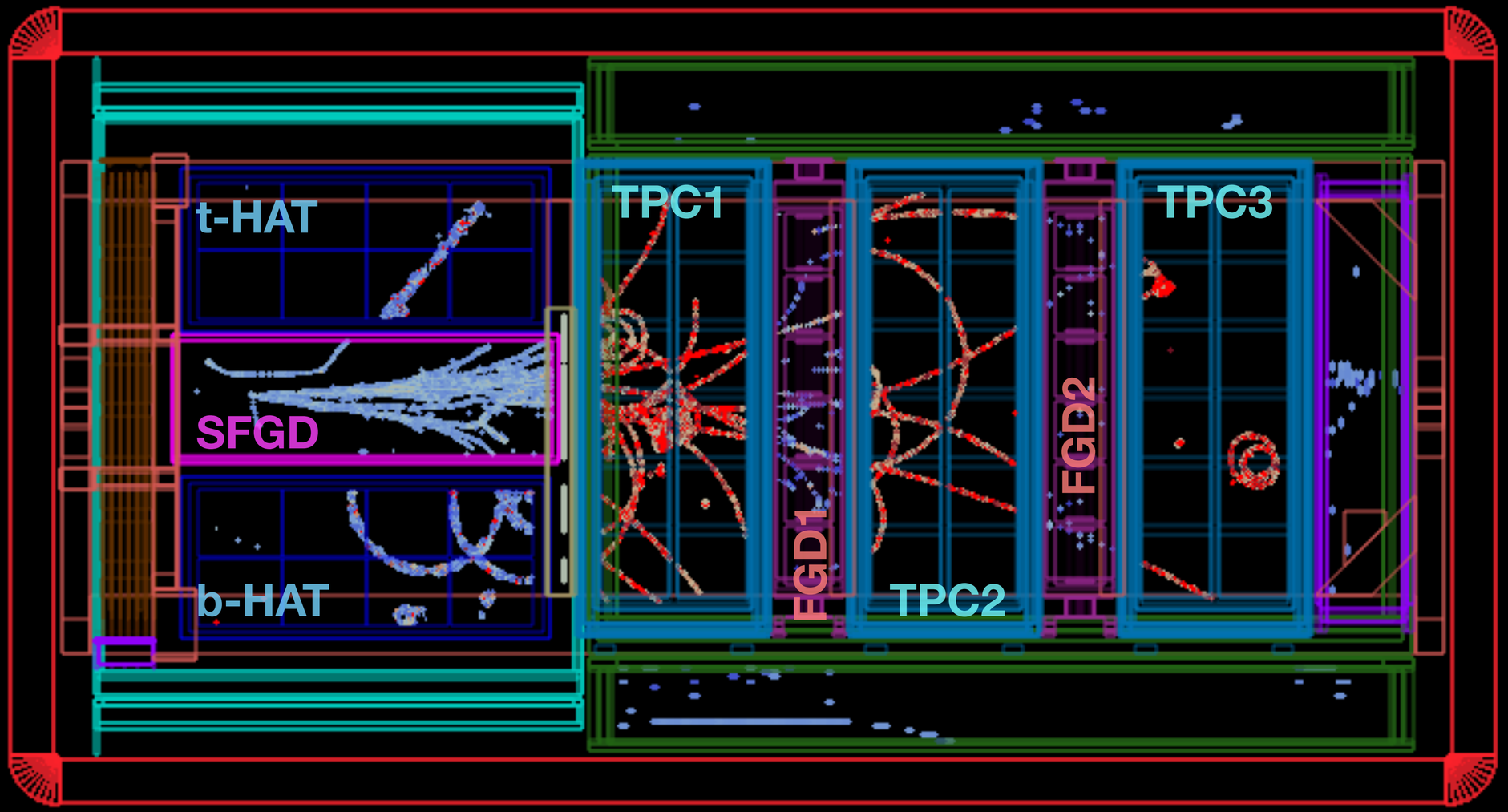

Thank you very much!
Cảm ơn nhiều!

Backup Materials

Tomislav Vladisavljevic, Rutherford Appleton Laboratory, UKRI
tomislav.vladisavljevic@stfc.ac.uk

On behalf of the T2K Collaboration
Given at 21st Recontres du Vietnam, 22-25 July 2025,ICISE, Quy Nhon, Vietnam

Science and Technology Facilities Council

Neutrino oscillations

- Mixing between distinct flavour eigenstates (interacting states) and mass eigenstates (propagating states), as governed by the **Pontecorvo-Maki-Nakagawa-Sakata matrix**

$$\begin{pmatrix} \nu_e \\ \nu_\mu \\ \nu_\tau \end{pmatrix} = \begin{pmatrix} 1 & 0 & 0 \\ 0 & c_{23} & s_{23} \\ 0 & -s_{23} & c_{23} \end{pmatrix} \begin{pmatrix} c_{13} & 0 & s_{13}e^{-i\delta_{CP}} \\ 0 & 1 & 0 \\ -s_{13}e^{i\delta_{CP}} & 0 & c_{13} \end{pmatrix} \begin{pmatrix} c_{12} & s_{12} & 0 \\ -s_{12} & c_{12} & 0 \\ 0 & 0 & 1 \end{pmatrix} \begin{pmatrix} \nu_1 \\ \nu_2 \\ \nu_3 \end{pmatrix}$$

Atmospheric & Accelerator | **Accelerator & Reactor** | **Reactor & Solar**

$s_{ij} = sin\ \theta_{ij}$
$c_{ij} = cos\ \theta_{ij}$

$\theta_{23} \approx 48^\circ$
$|\Delta m^2_{32}| \approx |\Delta m^2_{31}| \approx 2.5 \times 10^{-3}\ eV^2$

$\theta_{13} \approx 8^\circ$
$\delta_{CP} = ?$

$\theta_{12} \approx 34^\circ$
$\Delta m^2_{21} \approx 7.5 \times 10^{-5}\ eV^2$

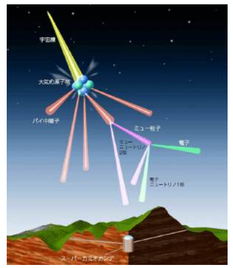


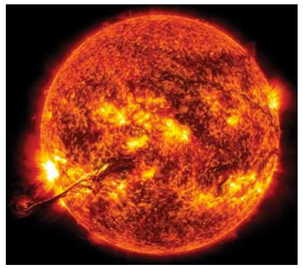

Oscillation probability, full expression from the CKM matrix

- Neutrino oscillations occur because of different flavour eigenstates (interacting states) and mass eigenstates (propagating states)

$\theta_{23} \approx 48^\circ$
$|\Delta m^2_{32}| \approx |\Delta m^2_{31}| \approx 2.5 \times 10^{-3}\ eV^2$

$\theta_{13} \approx 8^\circ$
$\delta_{CP} = ?$

$\theta_{12} \approx 34^\circ$
$\Delta m^2_{21} \approx 7.5 \times 10^{-5}\ eV^2$

$s_{ij} = sin\ \theta_{ij}$
$c_{ij} = cos\ \theta_{ij}$

$$\begin{pmatrix} \nu_e \\ \nu_\mu \\ \nu_\tau \end{pmatrix} = \begin{pmatrix} 1 & 0 & 0 \\ 0 & c_{23} & s_{23} \\ 0 & -s_{23} & c_{23} \end{pmatrix} \begin{pmatrix} c_{13} & 0 & s_{13}e^{-i\delta_{CP}} \\ 0 & 1 & 0 \\ -s_{13}e^{i\delta_{CP}} & 0 & c_{13} \end{pmatrix} \begin{pmatrix} c_{12} & s_{12} & 0 \\ -s_{12} & c_{12} & 0 \\ 0 & 0 & 1 \end{pmatrix} \begin{pmatrix} 1 & 0 & 0 \\ 0 & e^{i\lambda_{21}} & 0 \\ 0 & 0 & e^{i\lambda_{31}} \end{pmatrix} \begin{pmatrix} \nu_1 \\ \nu_2 \\ \nu_3 \end{pmatrix}$$

- Three flavour (anti)neutrino oscillation formula in vacuum:

$$P(\overset{(-)}{\nu}_\alpha \rightarrow \overset{(-)}{\nu}_\beta) = \delta_{\alpha\beta} - 4\sum_{k>j} Re\left\{U_{\alpha k}U^\star_{\beta k}U^\star_{\alpha j}U_{\beta j}\right\} sin^2\frac{\Delta m^2_{kj}L}{4E} \mp 2\sum_{k>j} Im\left\{U_{\alpha k}U^\star_{\beta k}U^\star_{\alpha j}U_{\beta j}\right\} sin\ 2\frac{\Delta m^2_{kj}L}{4E}$$

The T2K Off-Axis Neutrino Flux

- SK and ND280 are placed at 2.5° off-axis angle with respect to the primary proton beam direction
- On-axis near detector (INGRID) used to monitor beam stability and direction
- Off-axis beam makes the ν_μ flux more narrow and peaked around the energies needed for observing the first oscillation maximum at SK (295 km baseline)
- High energy tail gets reduced

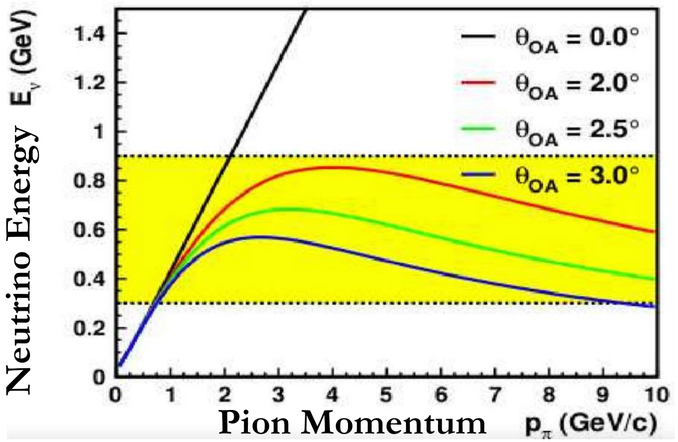

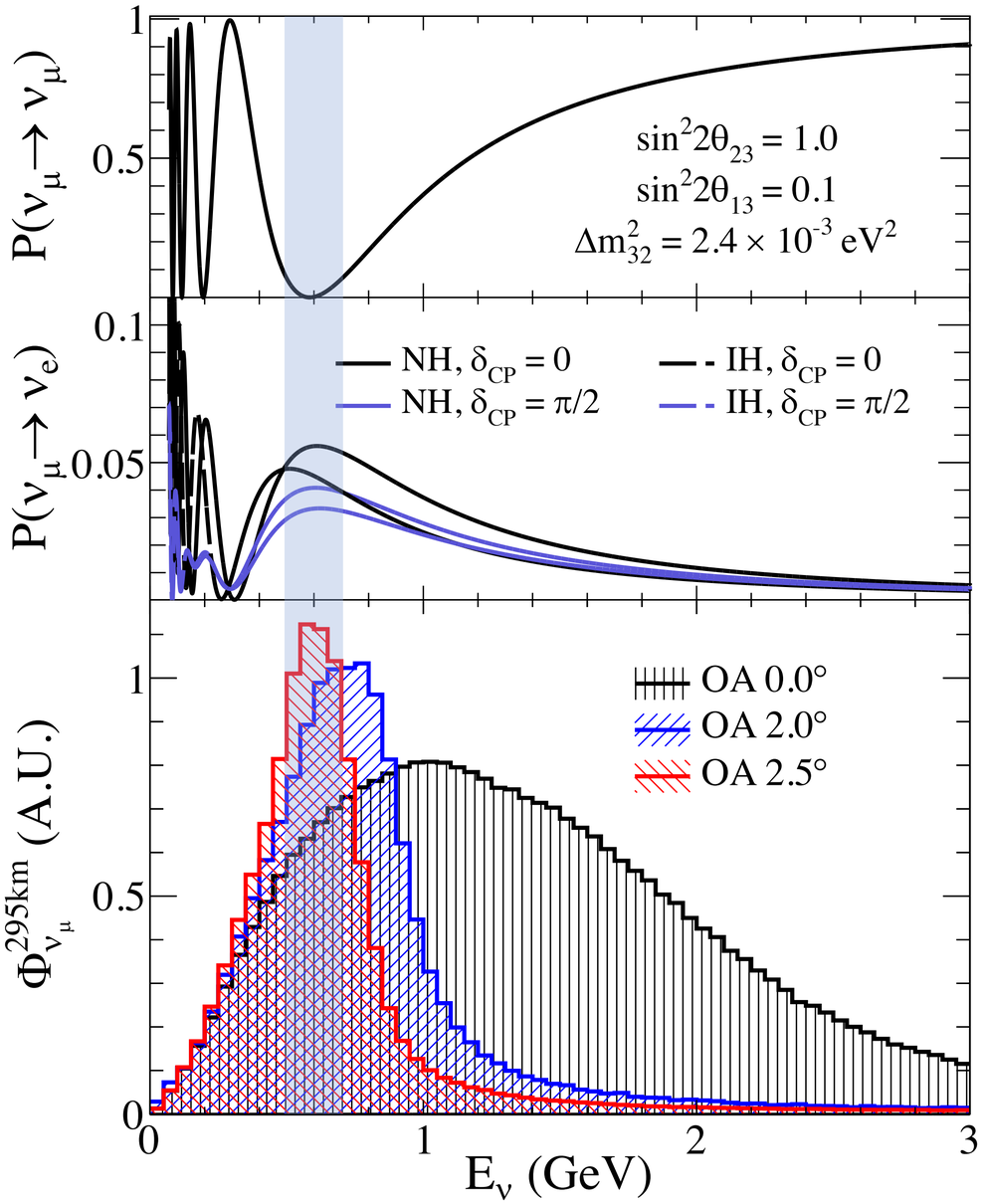

T2K's neutrino oscillation programme

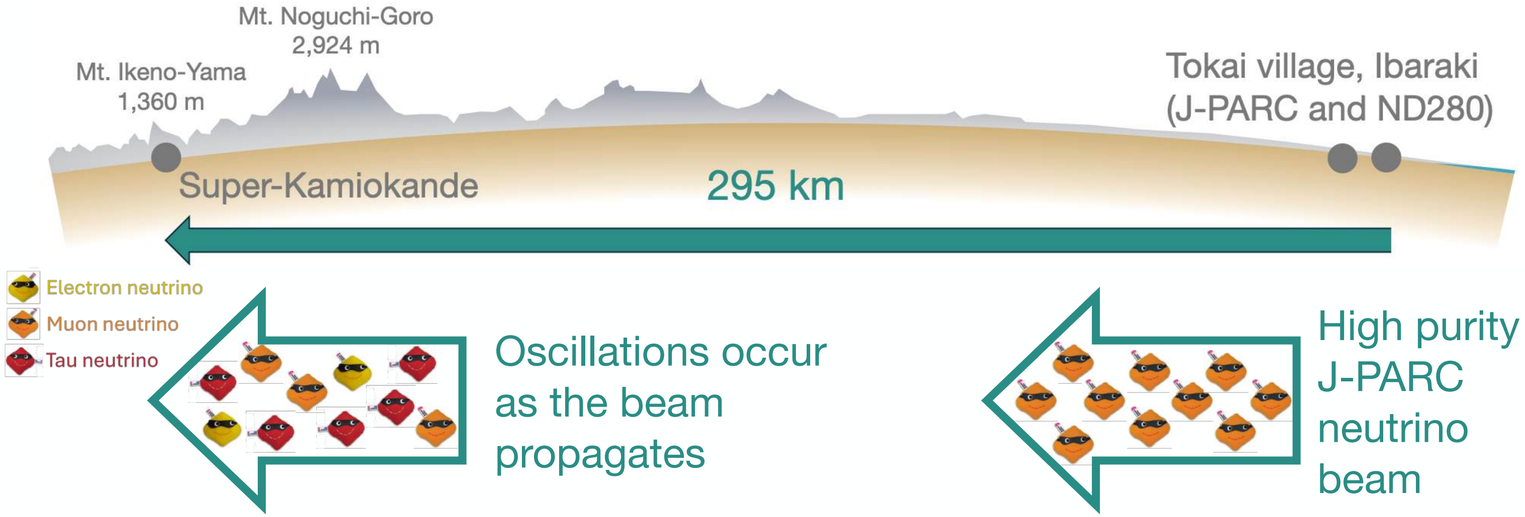

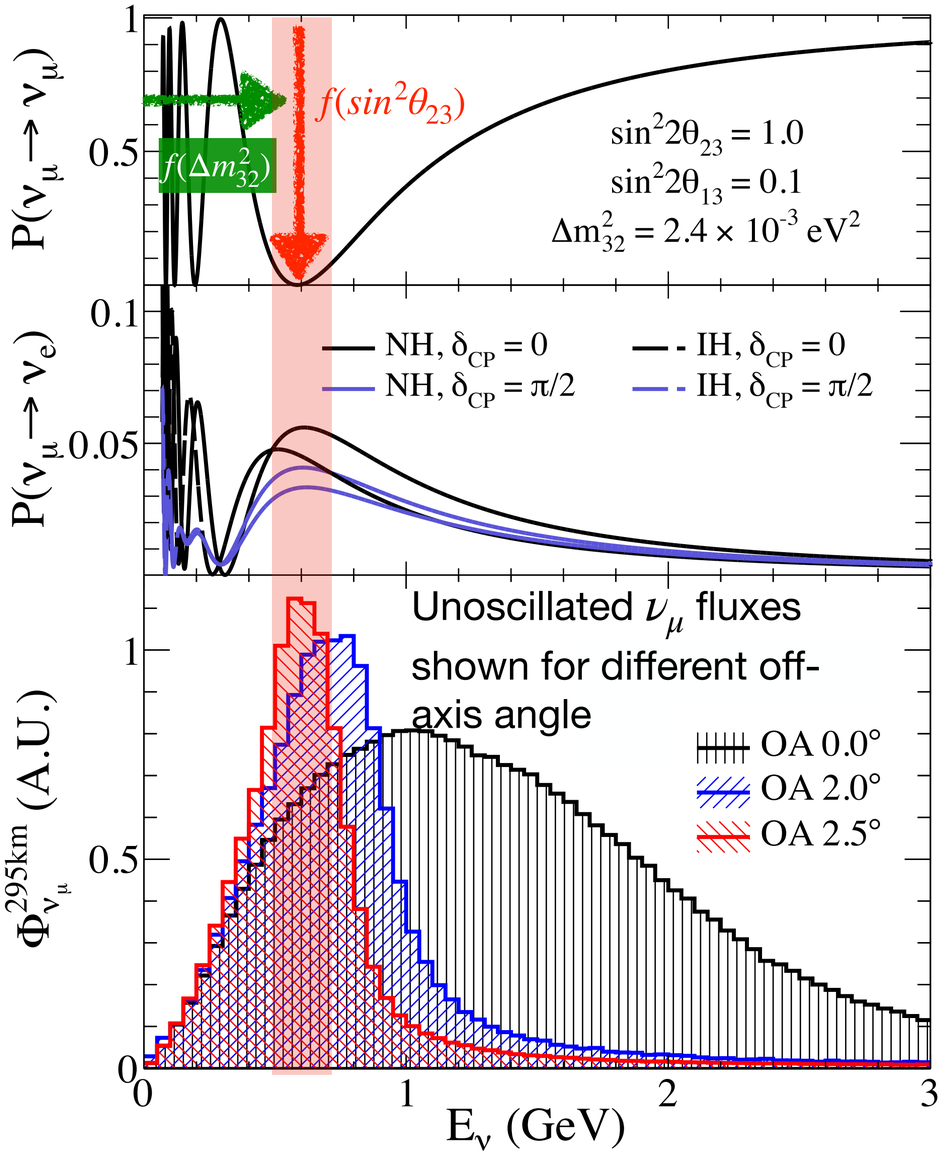

- T2K beamline can be configured to produce a high purity ν_μ (or $\bar{\nu}_\mu$) beam, with ND280 and Super-K located at 2.5 degrees off-axis wrt beam centre
- Minimum in $\nu_\mu(\bar{\nu}_\mu)$ survival after after 295 km is sensitive to Δm^2_{32} (via position of dip) and $sin^2\theta_{23}$ (via depth of dip)
- Appearance of $\nu_e(\bar{\nu}_e)$ after 295 km has sensitivity to δ_{CP} and the mass hierarchy

ν_e ($\bar{\nu}_e$) appearance probability at T2K

- Electron (anti)neutrino appearance probability:

$$P_{T2K}(\overset{(-)}{\nu}_\mu \rightarrow \overset{(-)}{\nu}_e) = \sin^2 2\theta_{13} \sin^2 \theta_{23} \sin^2 \frac{\Delta m^2_{32} L}{4E}$$

CP-conserving terms

$$+ \sin^2 2\theta_{13} \sin^2 \theta_{23} \sin^2 \frac{\Delta m^2_{21} L}{4E}$$

Can be neglected at L/E of long baseline accelerator experiments

$$+ J \cos\left(\frac{\Delta m^2_{32} L}{4E} \pm \delta_{CP}\right)$$

CP-violating term for $\delta_{CP} \neq 0, \pi$

Plus sign for neutrinos

where $J = \sin 2\theta_{12} \sin 2\theta_{23} \sin 2\theta_{13} \cos \theta_{13} \sin \frac{\Delta m^2_{32} L}{4E} \sin \frac{\Delta m^2_{21} L}{4E}$

ν_e ($\bar{\nu}_e$) appearance probability at T2K

- Electron (anti)neutrino appearance probability in vacuum:

CP-conserving term

$$P_{T2K}(\overset{(-)}{\nu}_\mu \rightarrow \overset{(-)}{\nu}_e) \approx \sin^2 2\theta_{13} \sin^2 \theta_{23} \sin^2 \frac{\Delta m^2_{32} L}{4E}$$

$$+ J \cos\left(\frac{\Delta m^2_{32} L}{4E} \pm \delta_{CP}\right)$$

Minus sign for $\bar{\nu}$

CP-violating term for $\delta_{CP} \neq 0, \pi$

- **The appearance probability gets modified** because of charged current ν_e coherent scattering from electrons in the Earth's crust

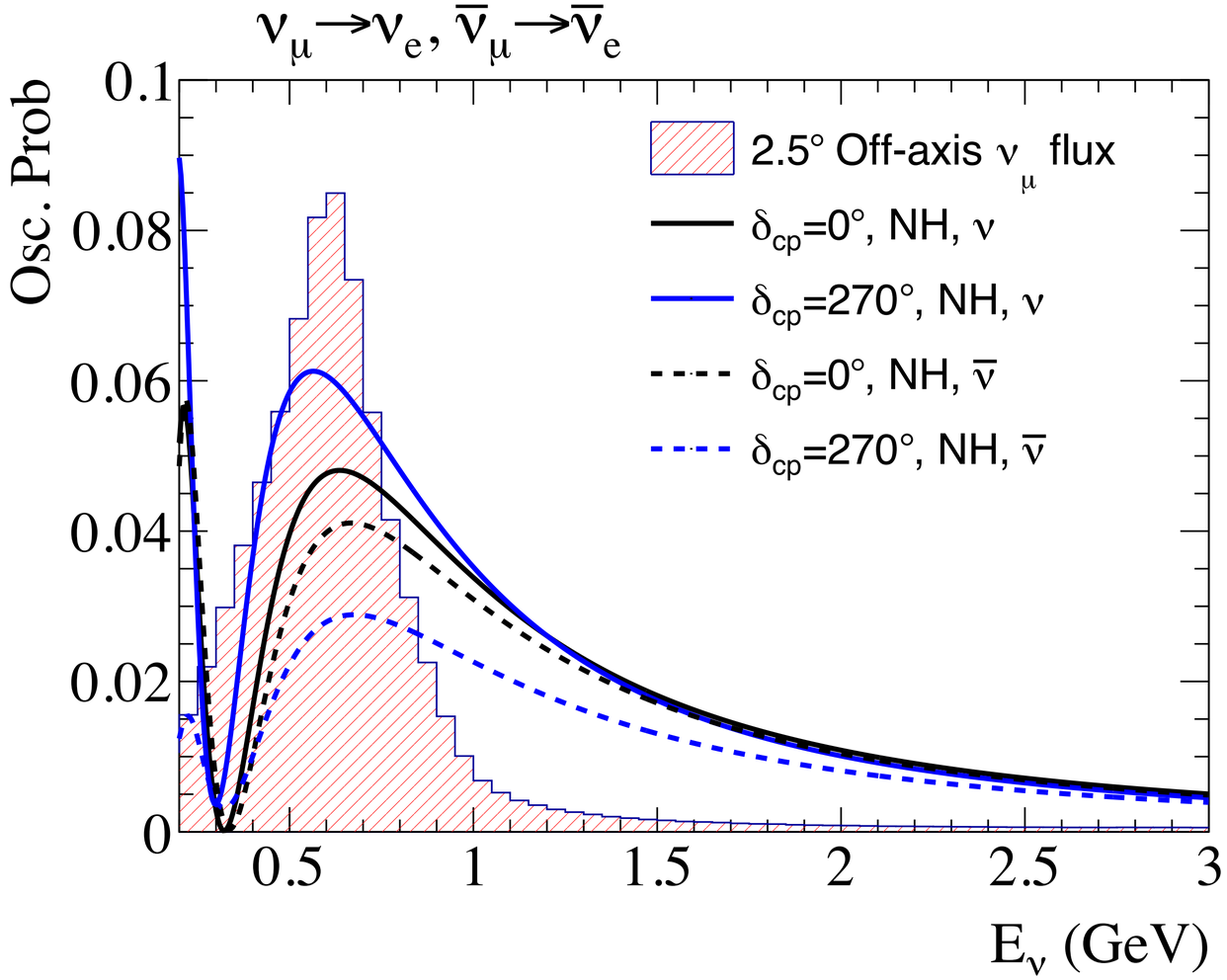

Appearance probability at T2K including matter effect

- Electron (anti)neutrino appearance probability around oscillation maximum:

Minus sign for anti-neutrinos

$$P_{T2K}(\overset{(-)}{\nu}_{\mu} \rightarrow \overset{(-)}{\nu}_{e}) \approx \sin^2 2\theta_{13} \sin^2 \theta_{23} \sin^2 \frac{\Delta m^2_{32} L}{4E} \left(1 \pm \frac{2a}{\Delta m^2_{31}} (1 - 2\sin^2 \theta_{13})\right)$$

$$\mp \sin 2\theta_{12} \sin 2\theta_{23} \sin 2\theta_{13} \cos \theta_{13} \sin \delta_{CP} \sin^2 \frac{\Delta m^2_{32} L}{4E} \sin \frac{\Delta m^2_{21} L}{4E}$$

Plus sign for anti-neutrinos

where $a = 2\sqrt{2}\, G_F\, n_e\, E$ depends on the electron density in Earth's crust n_e, and Fermi's constant G_F

ν_e ($\bar{\nu}_e$) appearance probability at T2K

- **The appearance probability gets modified** because of charged current ν_e coherent scattering from electrons in the Earth's crust

- **Mikheyev-Smirnov-Wolfenstein effect**

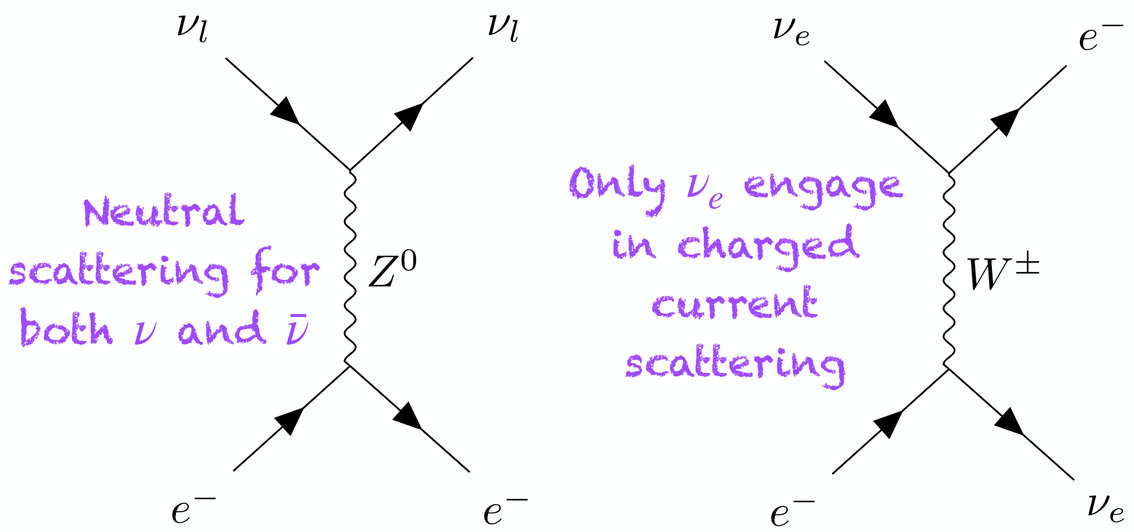

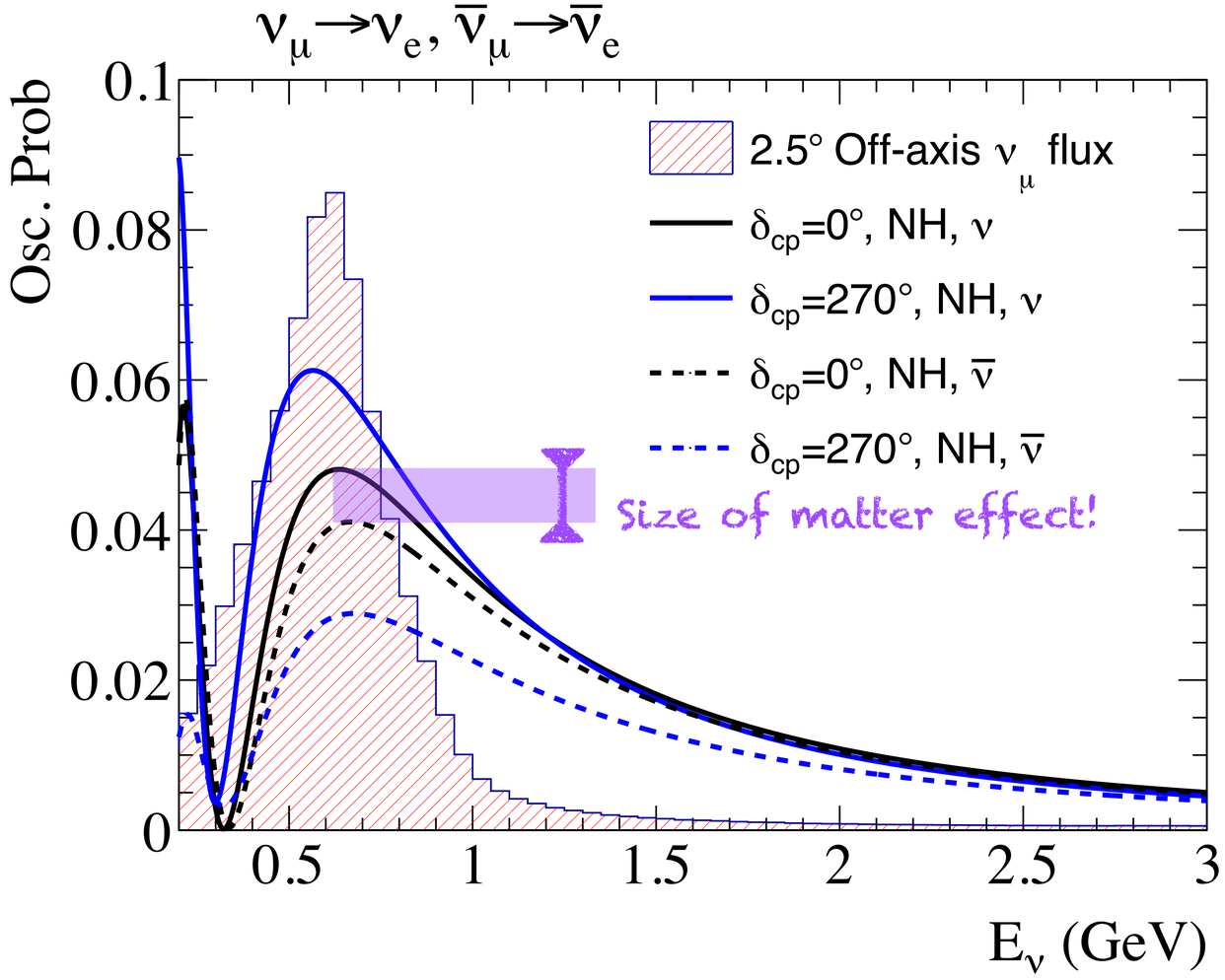

J-PARC facility

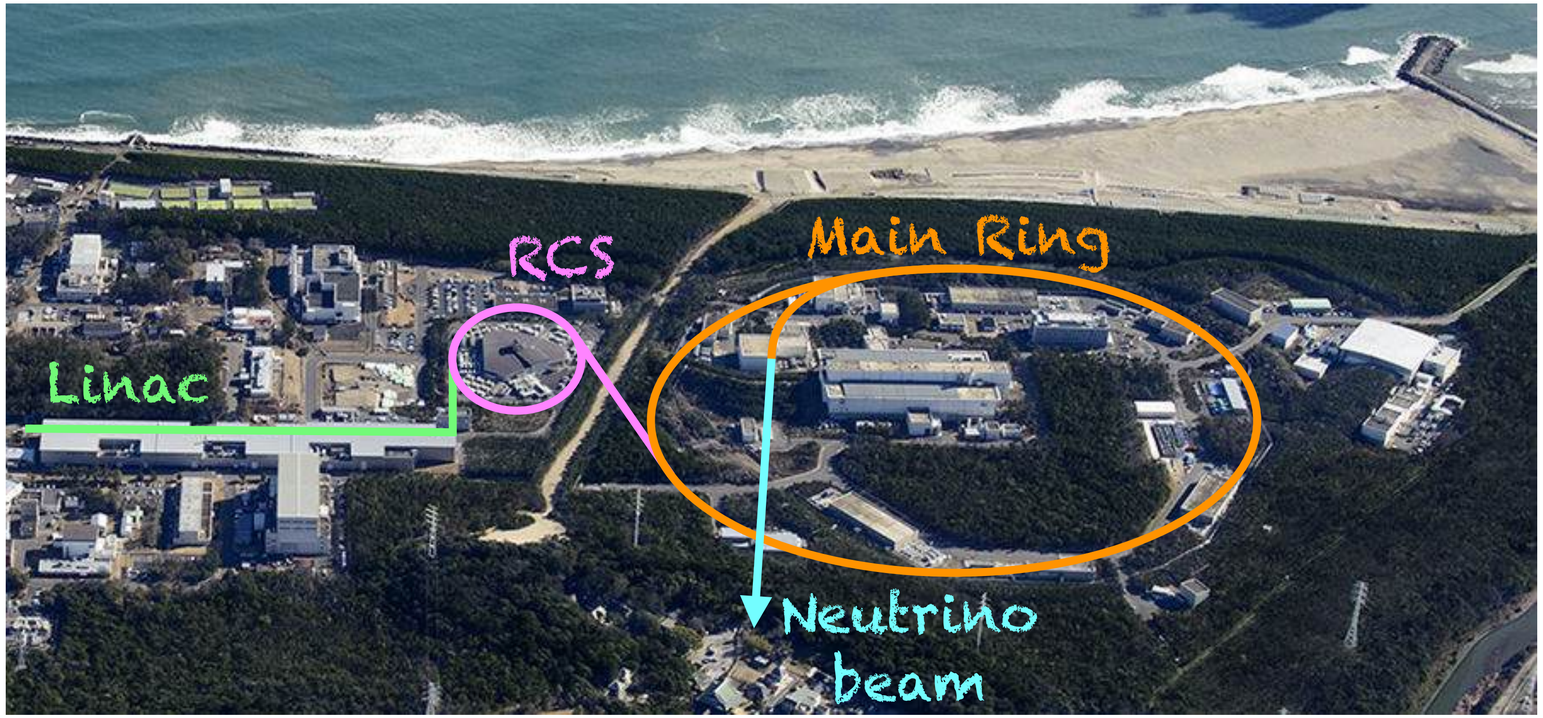

- 400 MeV Linac (H^-) to 3 GeV Rapid Cycling Synchrotron (p) to 30 GeV Main Ring (p) to 600 MeV Neutrino beam (ν)
- Low duty cycle for neutrino beam, so beam induced events are selected based on event timing

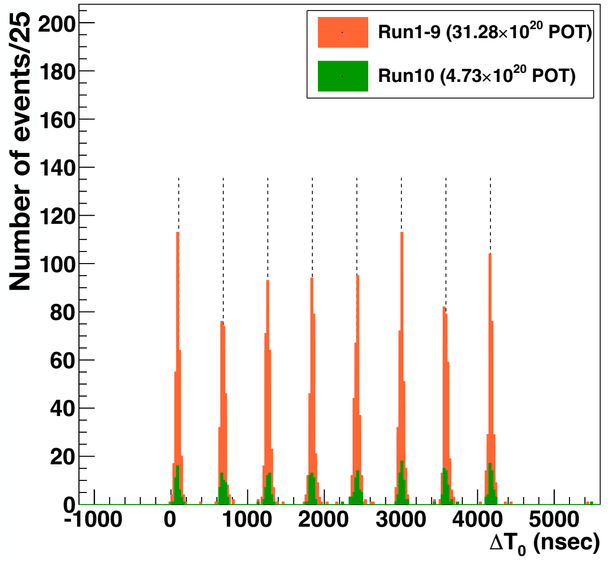

- 8 bunches per spill, with a spill repetition cycle of 2.48 s (now decreased to 1.38 s as part of the beamline upgrade)
- 80 ns bunch width, and 580 ns bunch separation

Secondary Beamline for T2K/Hyper-K

- 30 GeV (kinetic energy) protons striking the 90 cm long T2K graphite target
- Precise control of the **primary proton beam** is crucial for successful operation of T2K

- Theory of QCD is non-perturbative at these energies, thus not easily calculable

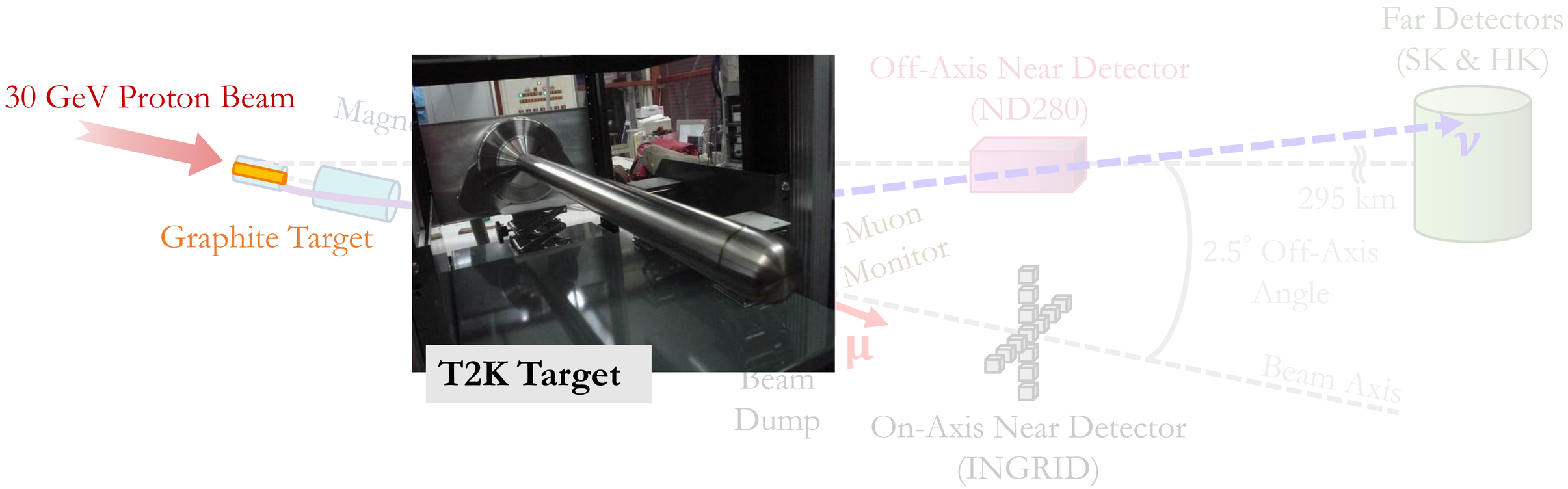

Tomislav Vladisavljevic (tomislav.vladisavljevic@stfc.ac.uk)

Secondary Beamline for T2K/Hyper-K

- Hadronic cascade is produced within the target (chain of hadronic interactions)

- 3 magnetic horns used to bend and (de)focus the pions and kaons exiting from the target, depending on their charge

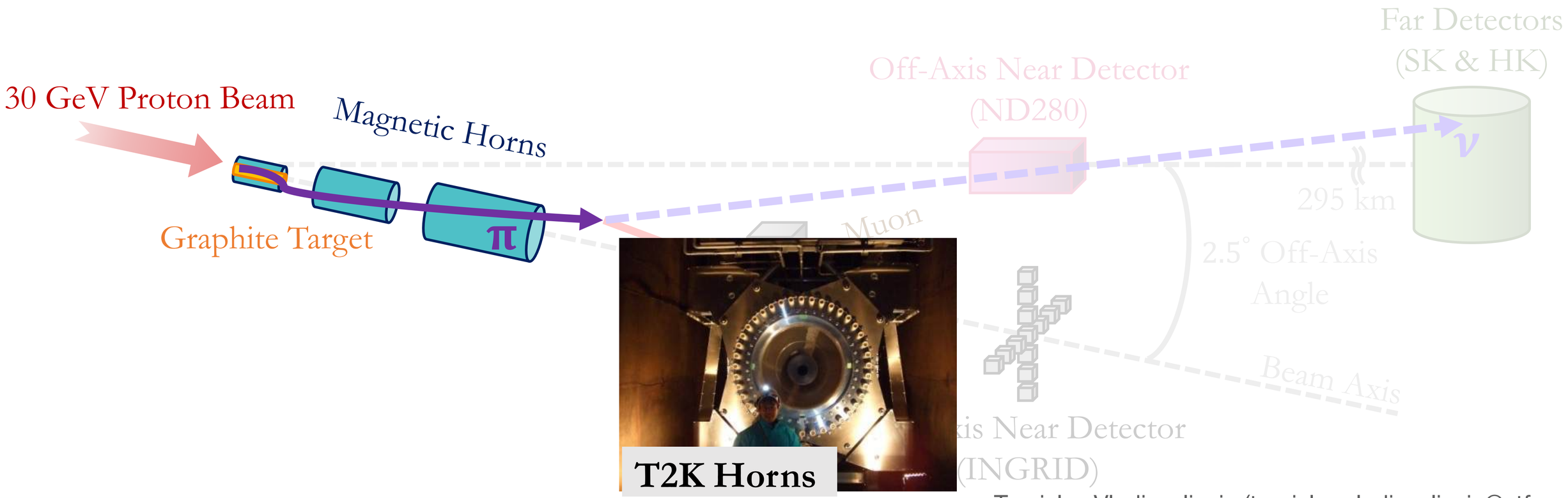

Tomislav Vladisavljevic (tomislav.vladisavljevic@stfc.ac.uk)

Secondary Beamline for T2K/Hyper-K

- Out-of-target interactions with secondary beamline components (horns, decay volume walls etc.) are important

- In-flight pion and kaon decays inside the decay volume (~96 m) produce neutrinos

$$\pi^+(K^+) \rightarrow \mu^+\nu_\mu$$

Signal

$$\mu^+ \rightarrow e^+\nu_e\bar{\nu}_\mu$$

Background

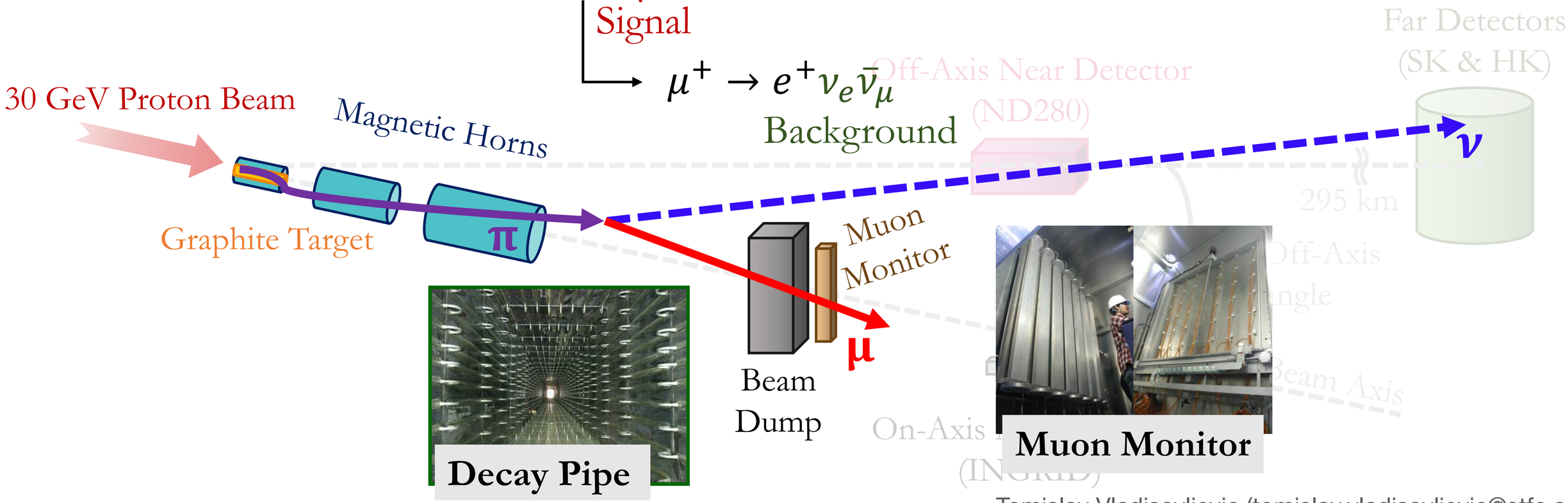

Tomislav Vladisavljevic (tomislav.vladisavljevic@stfc.ac.uk)

Secondary Beamline for T2K/Hyper-K

- Changing the horn current direction focuses either a neutrino (forward horn current) or an anti-neutrino (reverse horn current) enhanced beam towards the T2K detectors

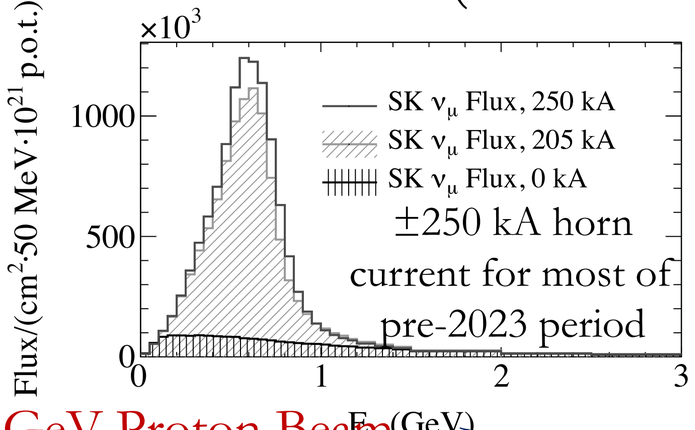

From 2023 operating horns at ±320 kA for 10% increase in flux

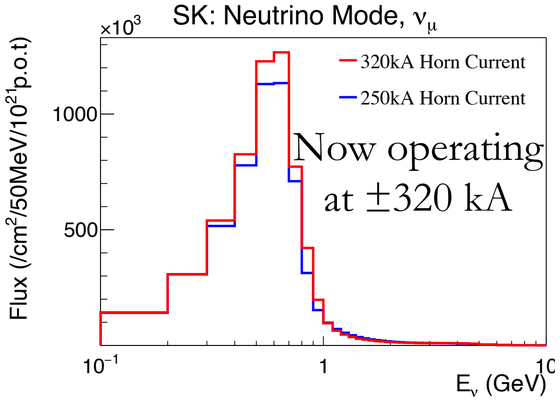

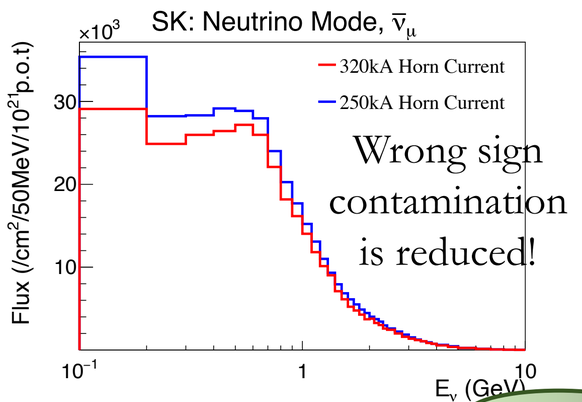

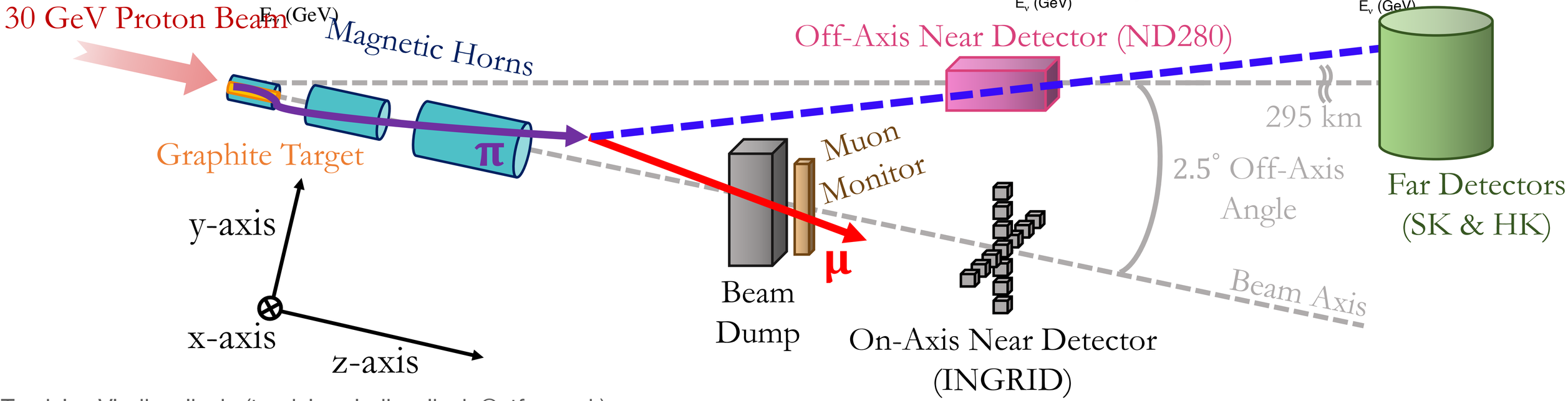

Tomislav Vladisavljevic (tomislav.vladisavljevic@stfc.ac.uk)

Particle identification at Super-K

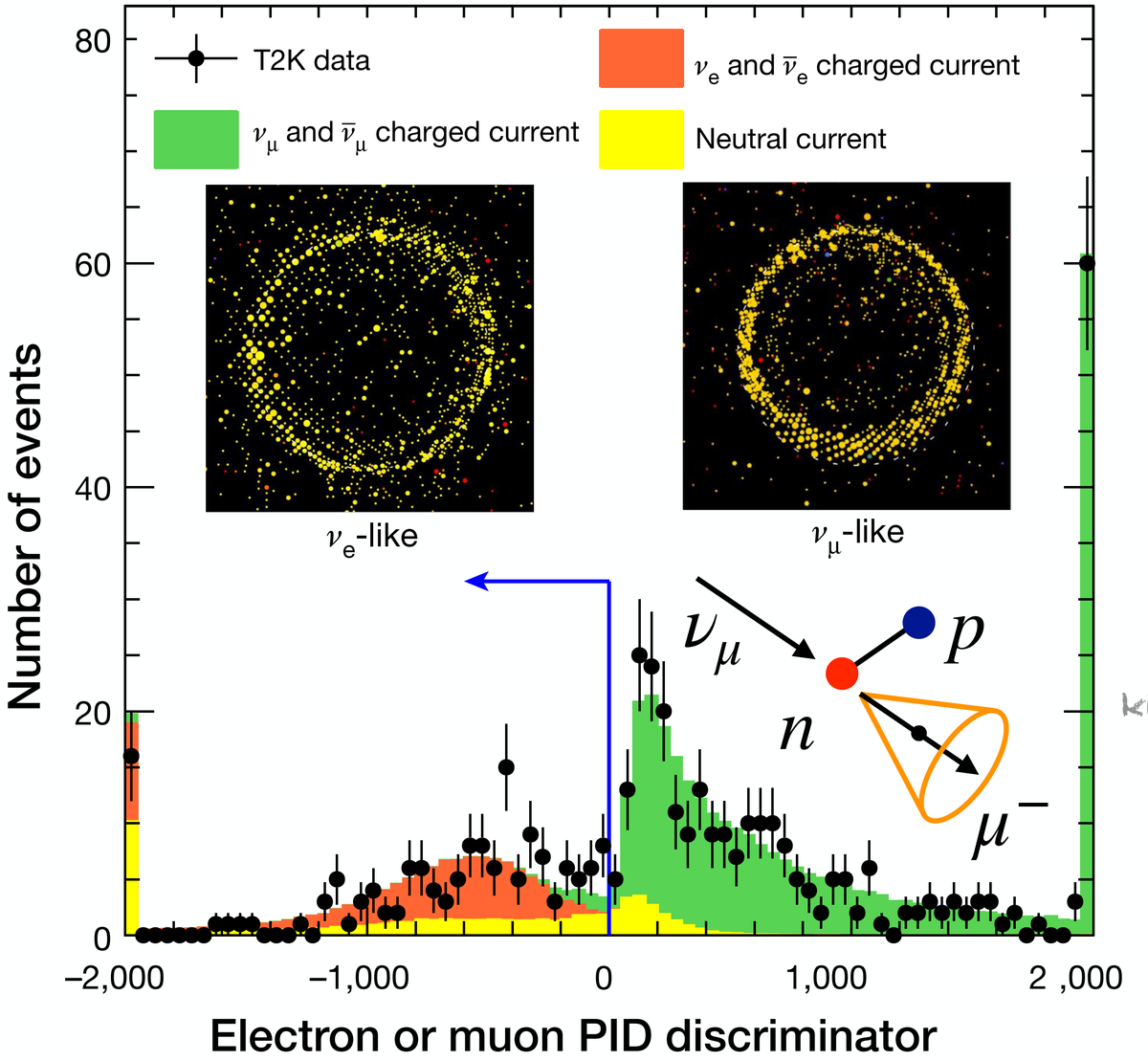

Electrons undergo more scattering, hence produce “fuzzy” Cherenkov rings

Good PID achieved using times, charge and position of all hit PMTs

Event topology hypothesis (1R muon-like, 1R electron-like etc.)

$$L(\Gamma,\theta) = \prod_{j}^{unhit\ PMTs} P_j(unhit\,|\,\Gamma,\theta) \prod_{i}^{hit\ PMTs} \left\{1 - P_i(unhit\,|\,\Gamma,\theta)\right\} \times f_q(q_i\,|\,\Gamma,\theta)\, f_t(t_i\,|\,\Gamma,\theta)$$

Event kinematics

Charge signal likelihood

Timing likelihood

$$PID = ln\left(\frac{L_\mu^{max}}{L_e^{max}}\right)$$

Tomislav Vladisavljevic (tomislav.vladisavljevic@stfc.ac.uk)

SFGD Timing Performance

Track time resolution

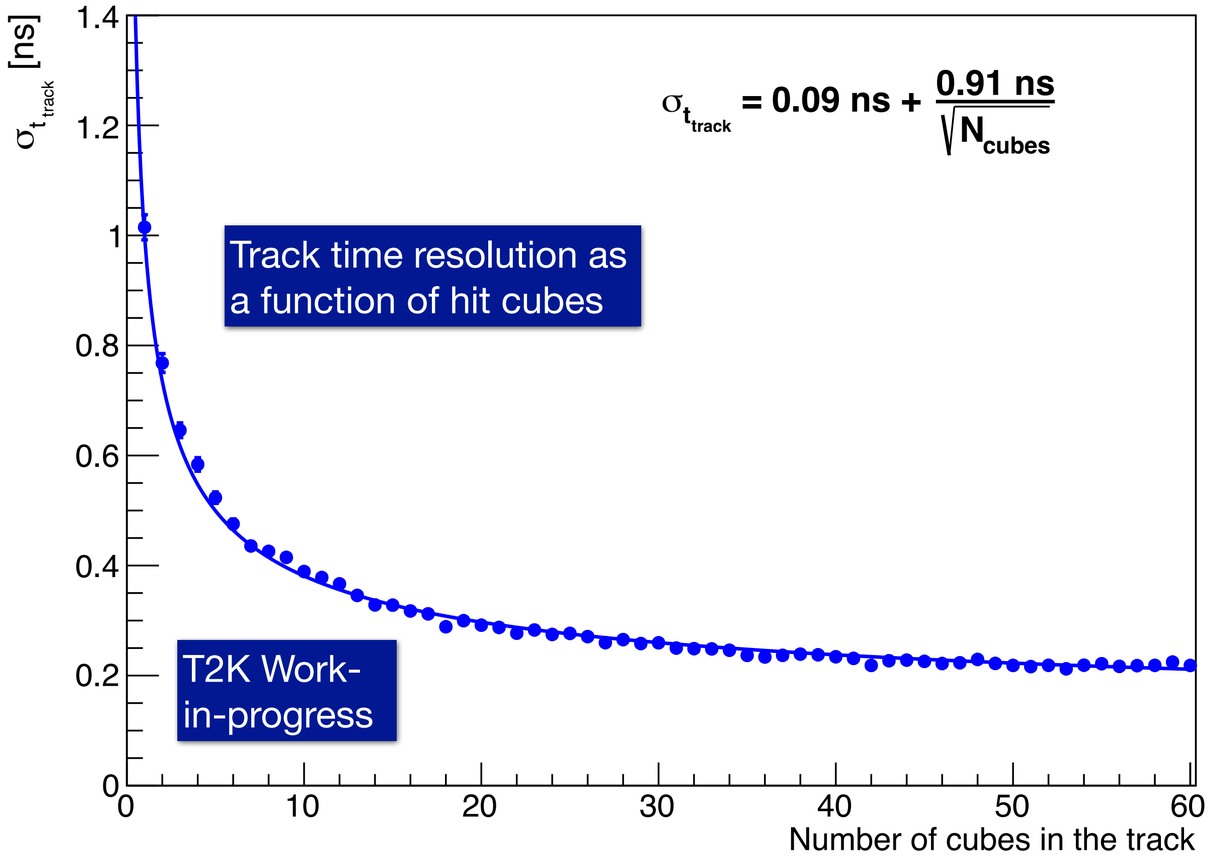

Cube time resolution

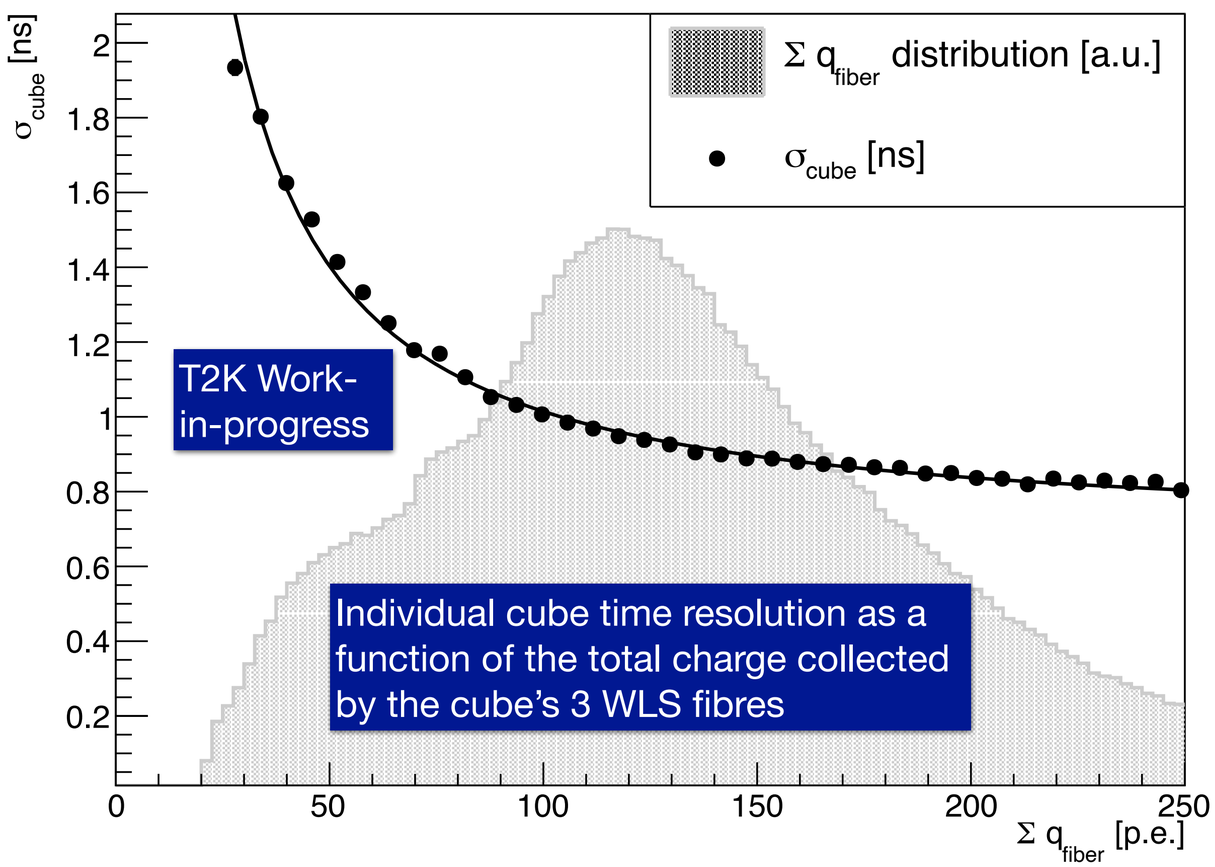

High Angle Time-Projection Chambers (HATs)

- Bottom and Top HAT detectors (each consisting of two Cu field cages) with uniform drift fields of ~275 V/cm, allow a close to 4π acceptance of tracks starting in SFGD

- Instrumented with the Encapsulated Resistive Anode MicroMegas (ERAM) technology which allows for charge spread across multiple anode pads (T2K is the first full scale experiment to use this, 8 ERAMs in every field cage)

Vertical TPC technology produces charge on single pads (600-1600 μm spatial resolution)

HAT allows for charge on multiple pads (200-800 μm spatial resolution)

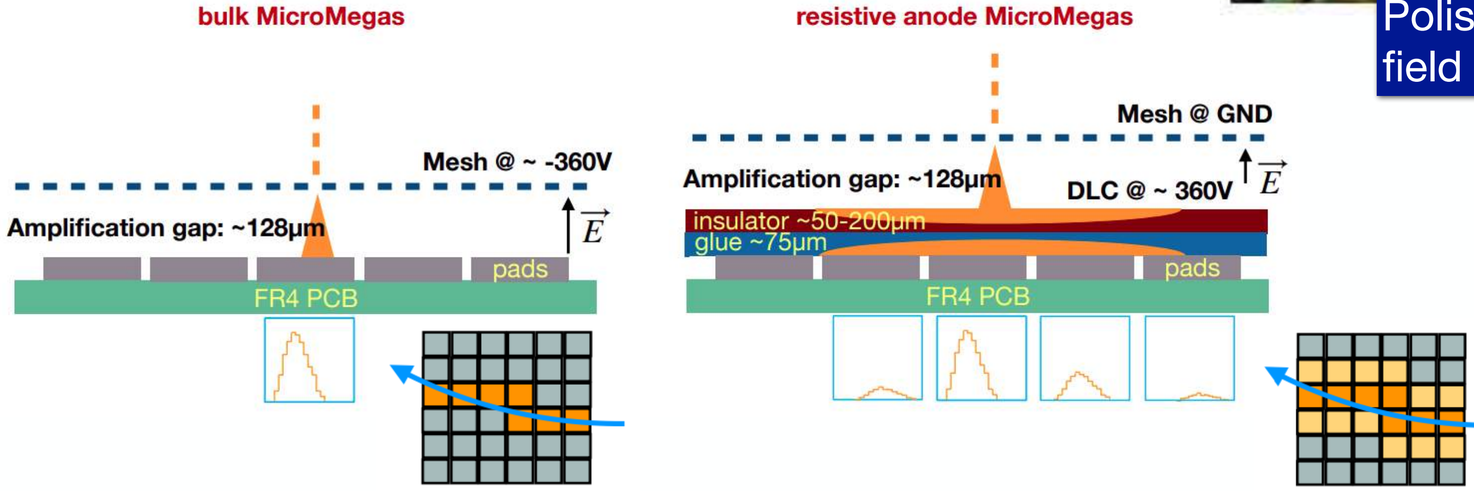

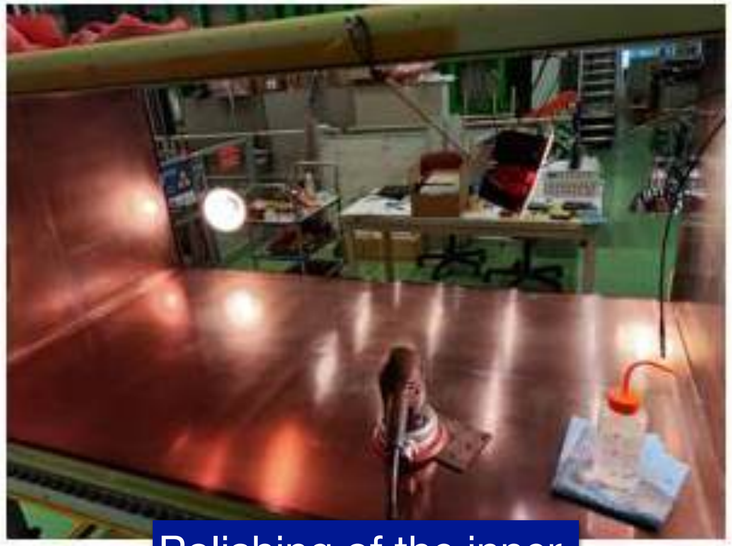

Polishing of the inner field cage surface

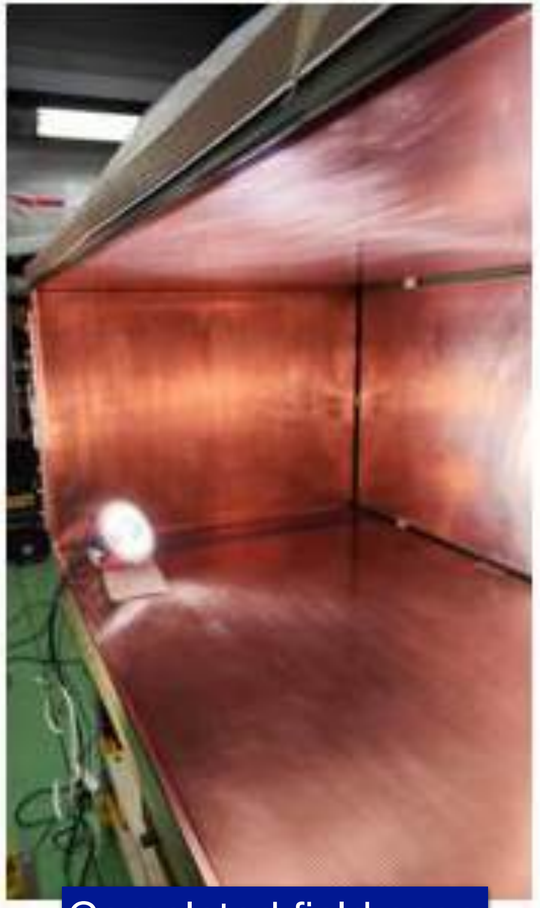

Completed field cage

For more details on characterisation of charge spread and gain with ERAMs refer to: arXiv:2303.04481

HAT performance from prototype commissioning at DESY

- The prototype was exposed to 1-4 GeV/c electron beams at DESY, and performance was assessed for different beam incident angles wrt to ERAMs, and for different drift distances

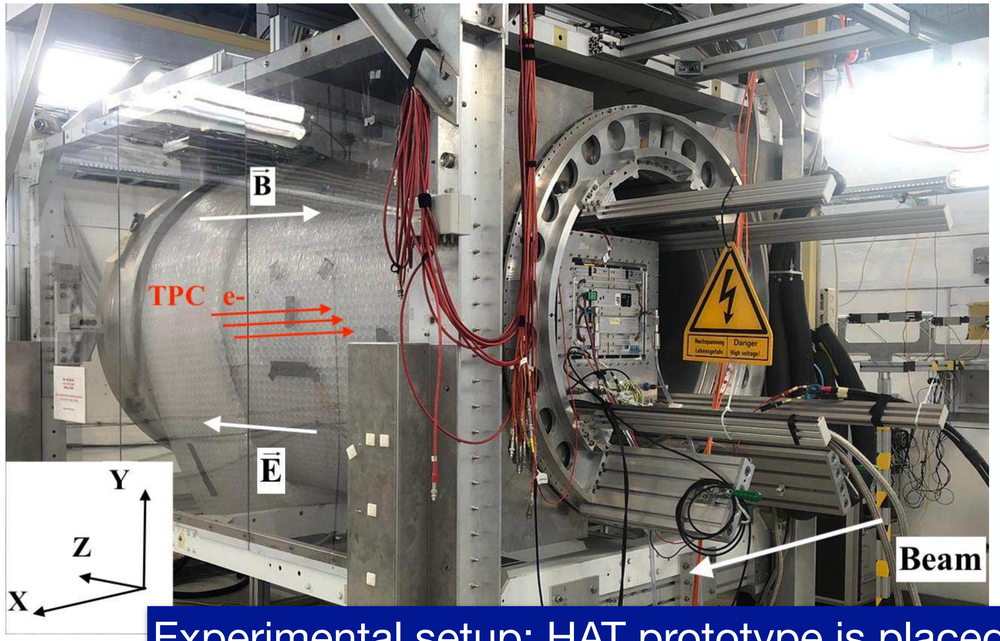

Experimental setup: HAT prototype is placed inside PCMAG solenoid, with a field up to 1.25 T

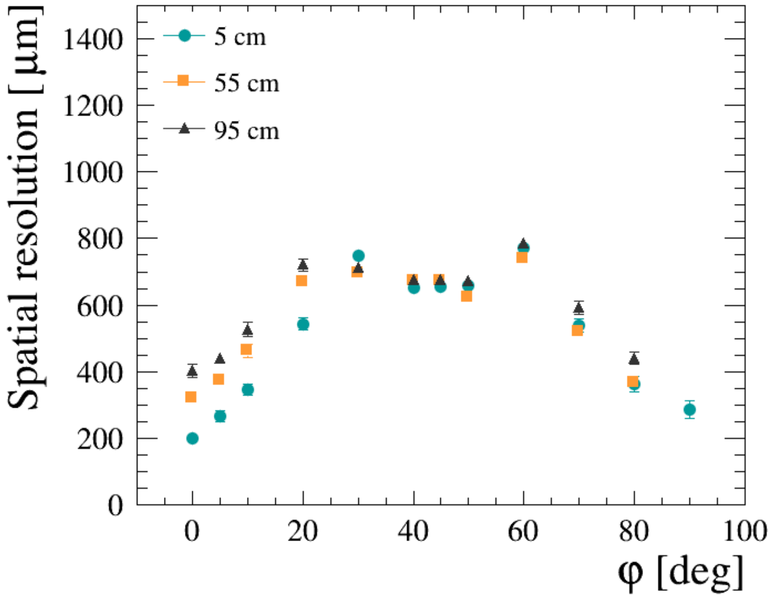

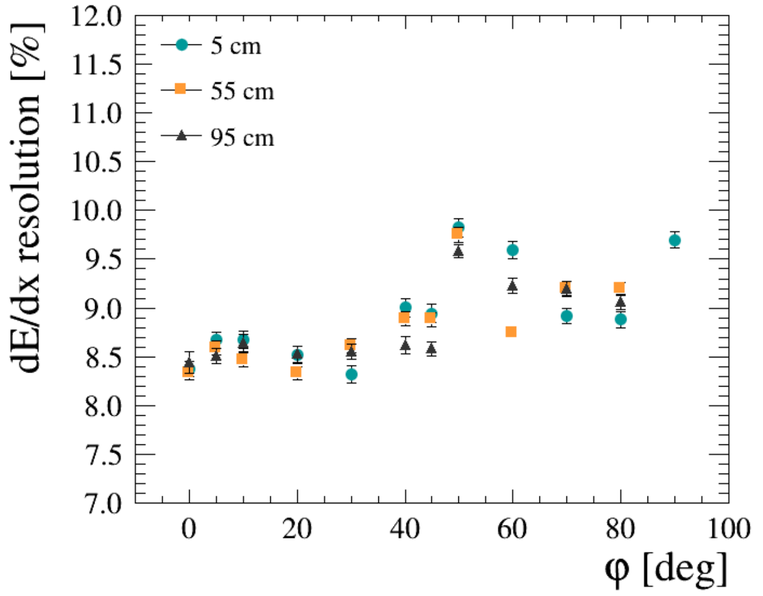

For more details on the HAT prototype performance, refer to:
Nucl. Instrum. Methods Phys. Res., A 1052 (2023) 168248

Time-of-flight (ToF) detectors

- Six ToF planes for a full enclosure of the SuperFGD target and HATs
- EJ-200 plastic chosen for its high light output, stable attenuation length, and fast timing (rise time of 0.9 ns)
- ToF bars: 1 cm thickness for good rigidity, 12 cm breadth for coupling to panels of 8 MPPC arrays, instrumented on either bar end
- 2 m long bars along beam, and 2.3 m long in perpendicularly facing upstream and downstream panels to accommodate basket size

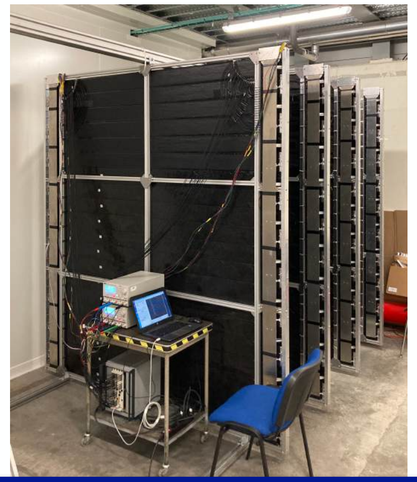

ToF panel commissioning at CERN

Assembly at CERN in ND280 basket prototype

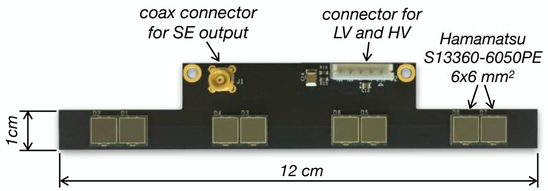

8 Hamamatsu MPPCs (S13360-6050PE) on each custom designed PCB

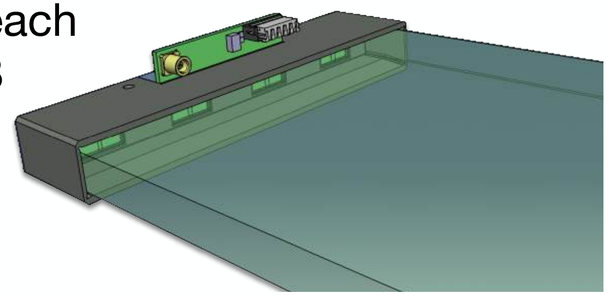

ToF performance

Results from performance test in CERN

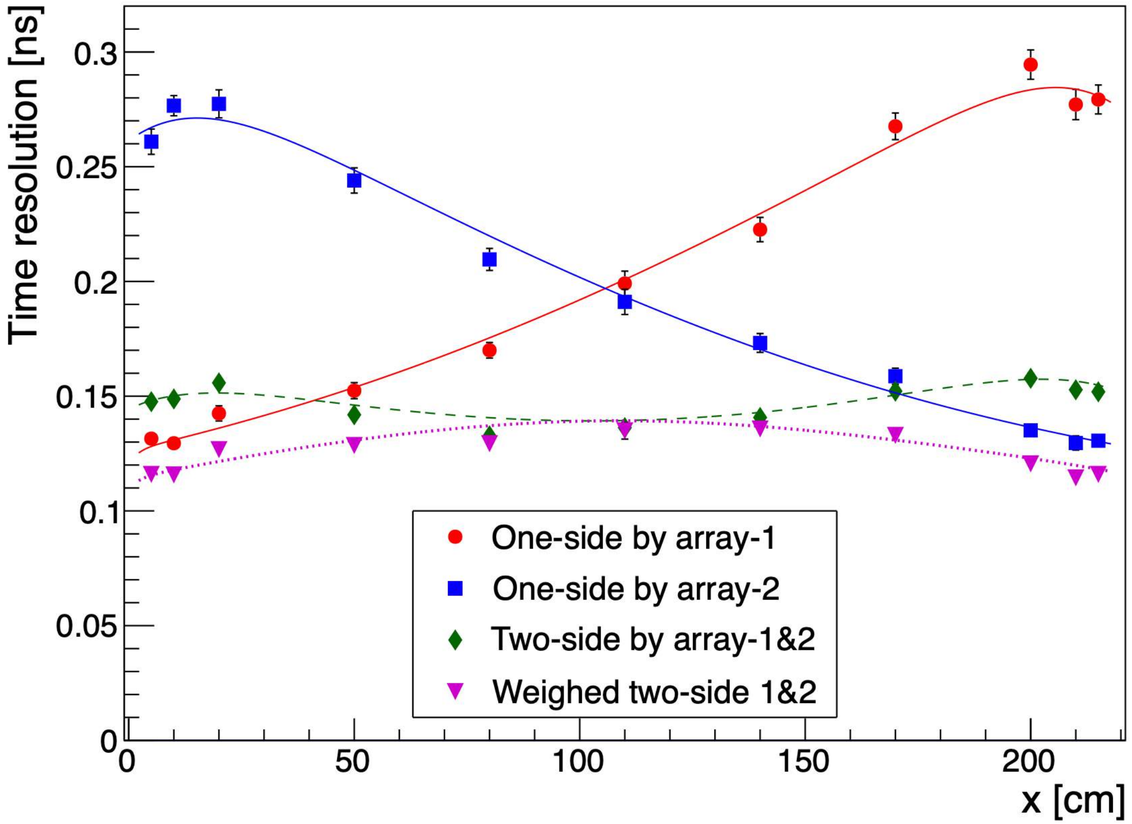

T2K's 8 bunch beam structure is clearly captured by the TOF panels

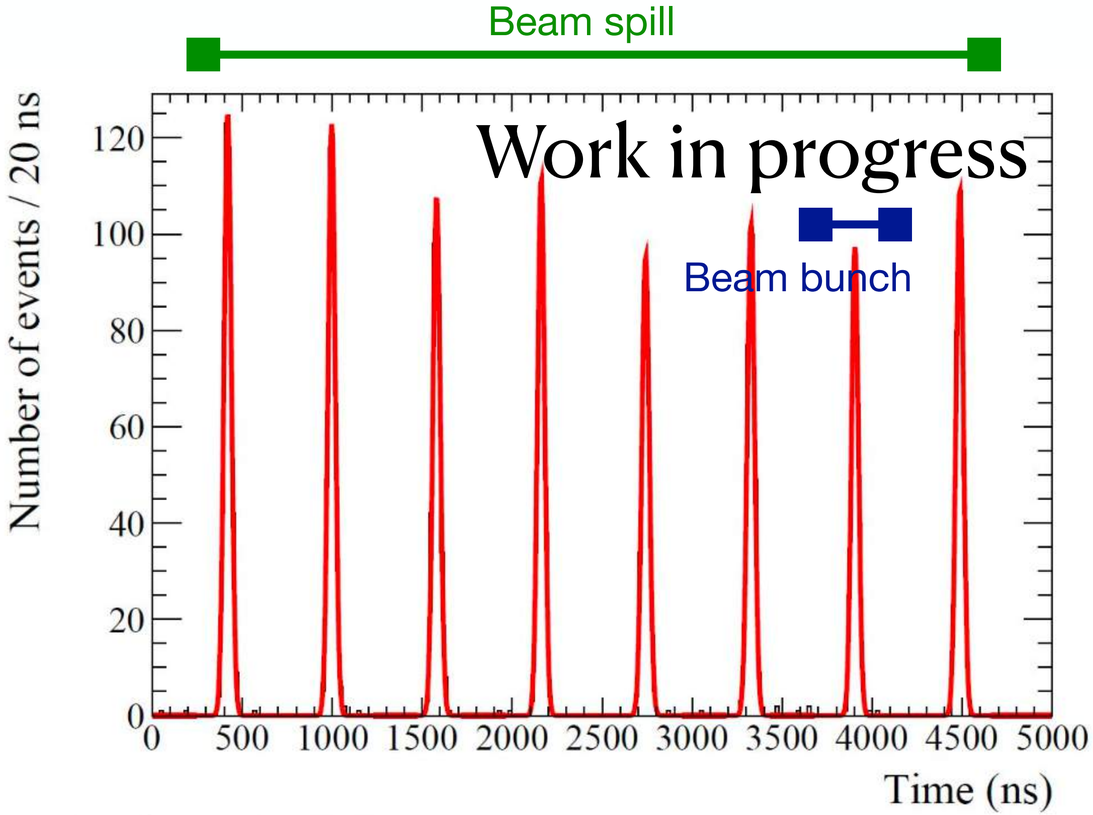

For more details on the ToF performance test at CERN, refer to: 2022 JINST 17 P01016

T2K oscillation analysis strategy: full overview

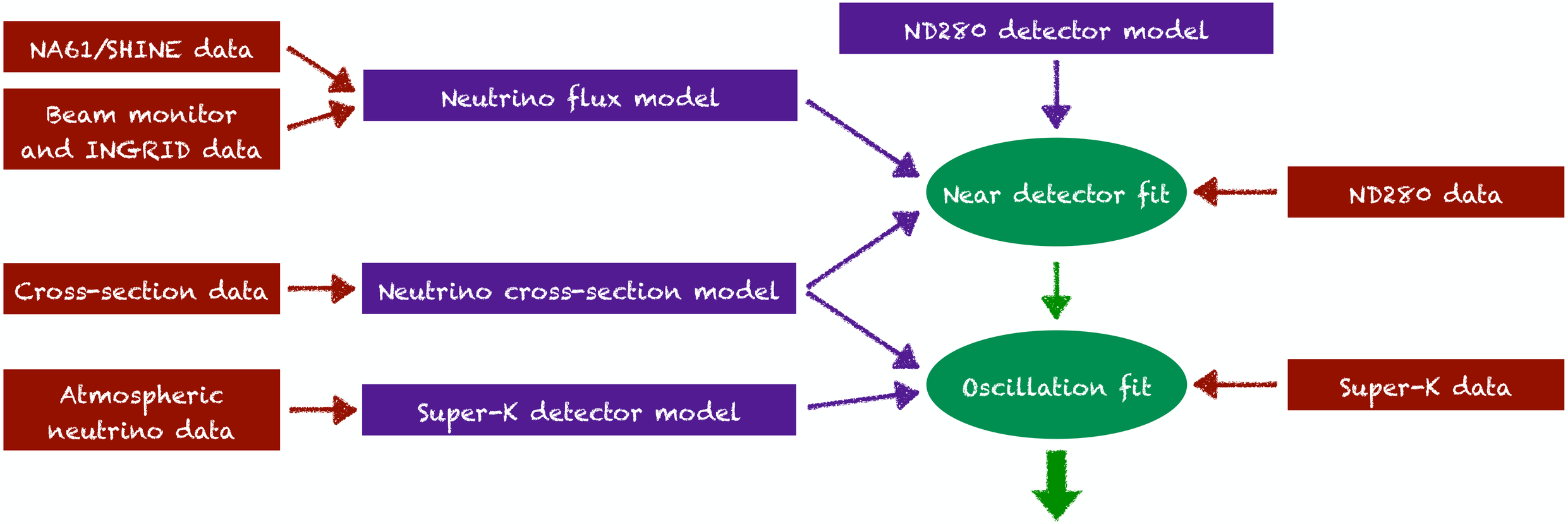

- **Frequentist** oscillation analyses: **first fit to near detector data, then fit to Super-K data**

T2K oscillation analysis strategy: full overview

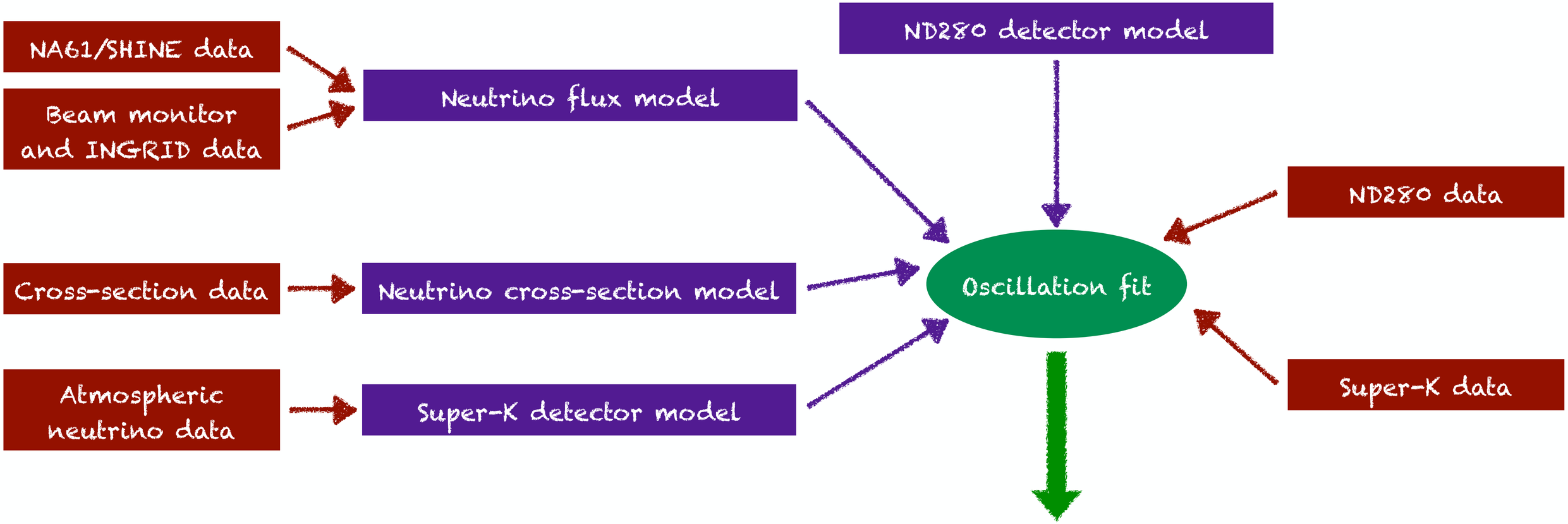

- **MaCh3 (Bayesian)** oscillation analysis: **simultaneous fit to near and far detector data**
- T2K produces consistently converging results from the simultaneous and sequential fitting approaches

T2K oscillation result!

Δm^2_{32}, $sin^2\,\theta_{23}$, δ_{CP}

Markov Chain Monte Carlo

- MCMC algorithm presents an efficient solution for sampling from a complex multivariate posterior likelihood distribution
- The algorithm provides a recipe for building the Markov chain
- At each step, an ensemble of model parameters is either accepted or rejected based on a comparison with a metric
- Parameters in the resulting Markov Chain have a distribution density proportional to the posterior likelihood

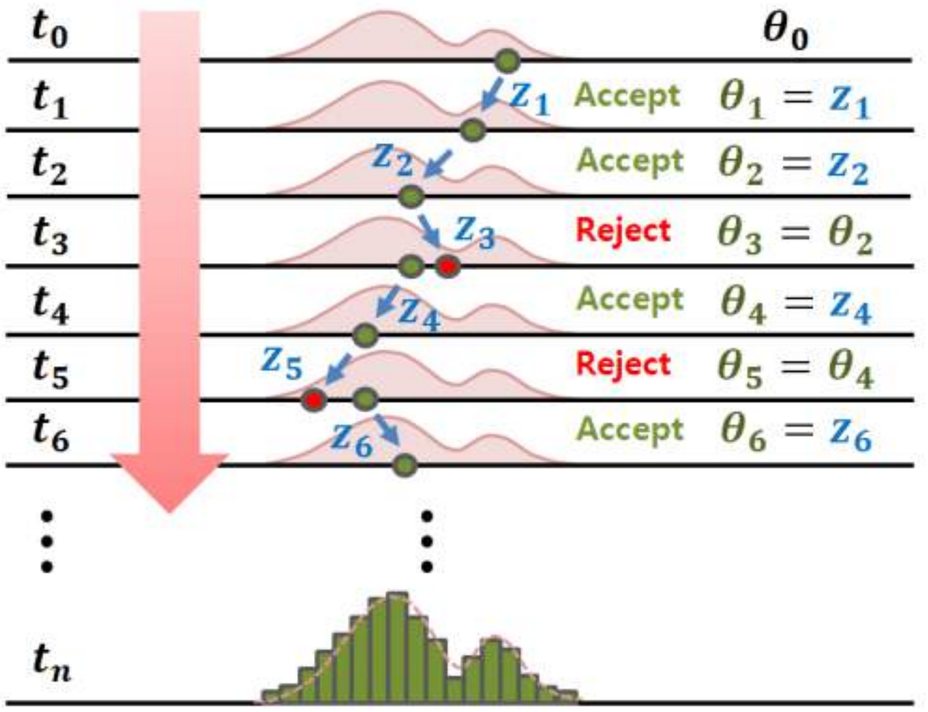

Figure from Adaptive Markov chain Monte Carlo algorithms for Bayesian inference: recent advances and comparative study

δ_{CP} and $sin^2\theta_{23}$ constraints from T2K

Confidence level	Interval (NH)	Interval (IH)
1σ	[-2.69,-0.75]	
90%	[-3.04,-0.34]	[-2.07,-0.91]
2σ	$[-\pi,-0.13] \cup [3.06,\pi]$	[-2.34,-0.67]
3σ	$[-\pi,0.43] \cup [2.54,\pi]$	[-2.92,-0.08]

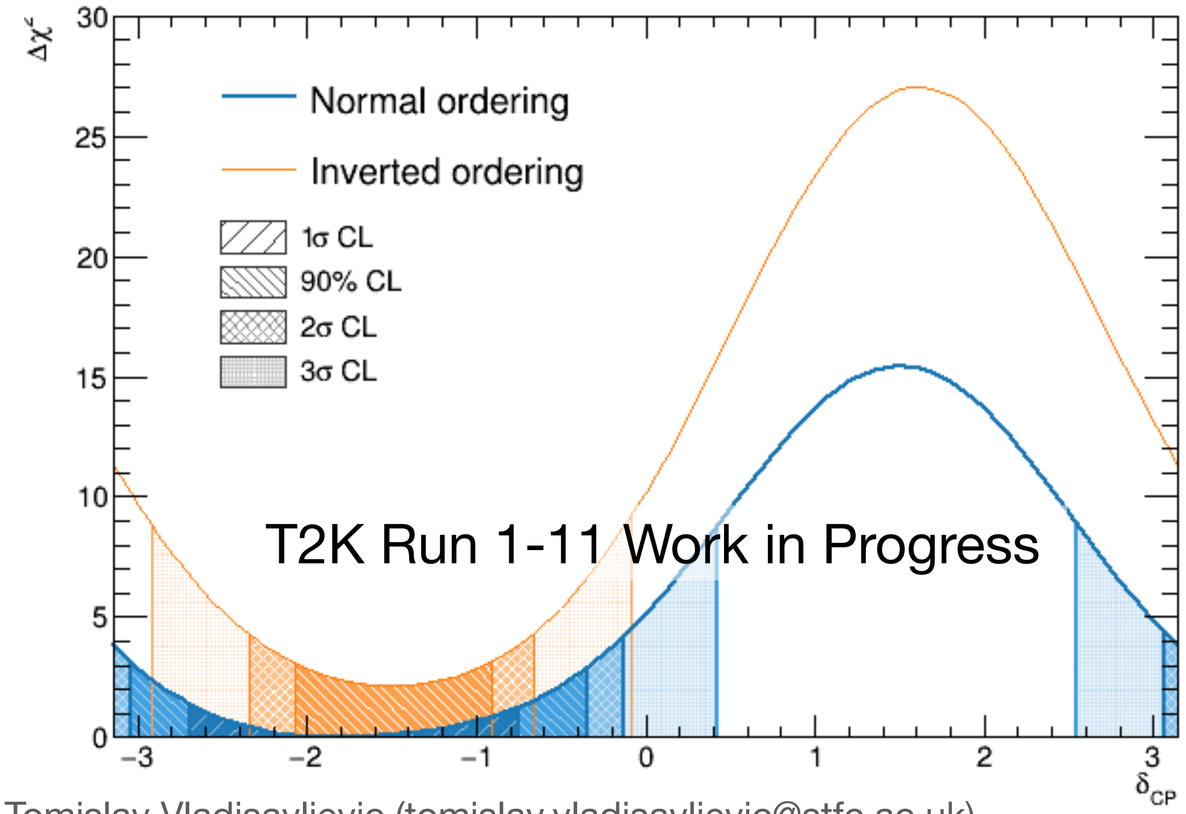

Confidence level	Interval (NH)	Interval (IH)
1σ	$[0.464,0.482] \cup [0.532,0.582]$	
90%	[0.443,0.592]	[0.530,0.586]
2σ	[0.436,0.598]	[0.466,0.592]